Studying the role of the AdeIJK RND efflux pump and its transcriptional regulator AdeN in the resistance and virulence of *Acinetobacter baumannii*

By: Mark Unger

A thesis submitted to the Faculty of Graduate Studies of The University of Manitoba in partial fulfillment of the requirements to the degree of

MASTER OF SCIENCE

Department of Microbiology
University of Manitoba

Acknowledgments

Firstly I would like to express my overwhelming gratitude to my supervisor Ayush Kumar for taking me on as a graduate student. I am hugely grateful for his advice, training and support as I developed as a student and a researcher. I cannot truly express how much I appreciate his help and mentorship.

I would also like to thank my committee members Dr. Ivan Oresnik and Dr. George Zhanel for their support and advice when difficulties arose with my project.

I also wish to express my gratitude to Dr. Patrick Chong, Stuart McCorrister, and Dr. Garrett Westmacott for their assistance with the proteomics sample preparation and data analysis and Dennis Labossiere for his invaluable help and expertise with lipid extraction and analysis.

I would especially like to thank all the past and current members of the Kumar Lab for being a part of such a fun and interesting work environment and for all their help with my project and training me in different techniques. Particularly Manu Singh, Dr. Rakesh Patidar, Vanessa Kornelson and Malaka De Silva you guys made the last two years way more fun than I could have ever imagined.

I also would like to thank the whole department of microbiology for making these last two years some of the most memorable of my entire life.

To my family, your support, encouragement and prayers have meant the world to me.

Lastly I would like to thank my amazing wife Ramina Unger, for supporting and encouraging me when I was tired or frustrated, and celebrating the victories when months of work finally paid off. I love you more than you will ever know.

Table of Contents

1 Abstract

Acinetobacter baumannii, a Gram-negative bacterium, is a problematic opportunistic pathogen due to its resistance to multiple antibiotics. Energy-dependent efflux of antibiotics mediated by proteins belonging to the Resistance-Nodulation-Division (RND) family is the predominant mechanism of intrinsic resistance in *A. baumannii*. AdeIJK is one such pump that is known to efflux a multitude to antibiotics in *A. baumannii*. AdeN, a TetR-family protein, has been previously shown to act as a repressor of the AdeIJK efflux pump. However, unlike other RND efflux pump regulators in *A. baumannii adeN* is not a linked to the *adeIJK* operon, it is instead located 813kbp upstream of the *adeIJK* efflux pump-encoding operon. Previous study by our group of the triclosan-resistant mutant AB042, which has a 73bp deletion in *adeN*, showed changes in the expression of a significant number of genes and proteins, indicating that AdeN may be acting as a global transcription regulator in *A. baumannii*. To study the role of AdeN, we have created an unmarked deletion mutant of *adeN* (AB141) in ATCC17978. Quantitative reverse transcriptase PCR in combination with transcriptomic and proteomic analysis was performed on AB141 to determine if AdeN is acting as a global transcription regulator. Biofilm formation, motility, virulence, antibiotic susceptibility, and microbial growth were also evaluated to assess the phenotypic effect of *adeN* deletion on *A. baumannii*. Transcriptomic and proteomic analysis of AB141 showed that *adeN* deletion results in differential expression of 106 genes greater than 1.5log(2) fold. Using a proteomics approach, we detected 31 proteins whose expression was altered greater than 1.5 fold. Phenotypic testing led to the observation that deletion of *adeN* results in decreased susceptibility to antibiotics and osmotic stress. The *adeN* deletion mutant also exhibited attenuated virulence, decreased biofilm formation and motility. In order to determine if the observed phenotypes were a result of overexpression of AdeIJK rather than loss of AdeN expression, an *adeIJK* deletion mutant (AB185) and a double mutant of *adeN*

and *adeIJK* (AB186) were created in ATCC17978 background and phenotypically evaluated alongside the *adeN* mutant AB141. Intriguingly both *adeIJK* deletion mutants also exhibited attenuated virulence and motility compared to wild-type. These data indicate that AdeN likely plays a much larger role as a global regulator in *A. baumannii* with respect to resistance and virulence, however the interactions between AdeN and AdeIJK are much more complicated than originally thought.

List of Tables

List of Figures

2 Introduction

2.1 Acinetobacter baumannii

Acinetobacter baumannii is a Gram-negative coccobacillus that is becoming one of the most significant, clinically-relevant organisms causing opportunistic multi- and pandrug resistant infections in immunocompromised individuals (Jain and Danziger 2004, Gordon and Wareham 2010). It was initially brought into the spotlight when it was determined to be of the major causes of infections of soldiers returning from conflicts in Iraq and Afghanistan (Tien et al. 2007). Since then, it has emerged as a significant nosocomial pathogen in hospitals around the world (Chuang et al. 2009, Apisarnthanarak and Mundy 2009). Most frequently associated with ventilator acquired pneumonia and catheter associated urinary tract infections (Michalopoulos and Falagas 2010), *A. baumannii* is able to survive the harsh hospital environments due to its ability to form biofilms and its high intrinsic resistance to antibiotics.

The multidrug resistant phenotype exhibited by *A. baumannii*, in combination with its ability to persevere in the hospital environment and cause infections, has led the Centers for Disease Control and Prevention (CDC) to classify *A. baumannii* as a threat level 'Serious' organism that 'requires immediate and sustained action to keep the organism under control' (*Antibiotic Resistance Threats in the United States* 2013). *A. baumannii* was also recently identified by the United Nations Health Agency and the World Health Organization as a critical threat to human health that requires immediate action with regards to research and development of new antimicrobials to counteract (*WHO | Global priority list of antibiotic-resistant bacteria to guide research, discovery, and development of new antibiotics* 2017).

2.2 Antibiotic Resistance

2.2.1 History of Antibiotic Discovery

Since the accidental discovery of penicillin by Alexander Fleming in 1928, antimicrobials have become likely the most successful chemotherapy in medical history. Before the advent of the antibiotic era infectious diseases were one of the leading causes of human death world-wide. However, despite penicillin being heralded as the first antibiotic ever discovered, research has shown that exposure to antimicrobials is not confined to the 20th and 21st centuries.

Due to the uniquely strong chelating properties exhibited by tetracyclines, which results in incorporation into bone and tooth enamel during exposure, archeological studies have been able to detect traces of tetracycline in bones from as early as 350-550 CE in Sudan (Bassett et al. 1980, Nelson et al. 2010) and Roman period Egypt (Cook et al. 1989).

While other antibiotics are much more difficult to detect in ancient samples, study of ancient healing customs and traditions have led to the discovery of many antimicrobials and antimicrobial producing organisms. These types of studies led to the discovery of the potent anti-malarial drug artemisinin which is extracted from the *Artemisia* plant, a plant that has been used in traditional Chinese medicine for thousands of years (Cui and Su 2009). Other traditional Chinese medicines have also been shown to exhibit antimicrobial activity and further study could lead to the discovery of further antimicrobials (Wong et al. 2010). Following anecdotal evidence of the healing properties of red soils in Jordan for treating skin infections, researchers have been led to the discovery of a number of antibiotic producing bacteria such as actinomycetes, which produce the transcription inhibitor actinomycin, in these soils (Falkinham et al. 2009). However, as we now understand all too well, use of antimicrobials results in selective pressure for the accumulation of antimicrobial resistance determinants and the fact that these pressures have been

in place for thousands of years, as opposed to only for the last hundred, is a cause for increased concern as to the continued effectiveness of our current antibiotic arsenal (Aminov and Mackie 2007, Kobayashi et al. 2007).

While the concept of antibiotic chemotherapy is largely attributed to Paul Ehrlich and his "magic bullet" hypothesis, that chemical compounds could be synthesized that would "be able to exert their full action exclusively on the parasite harbored within the organism" (Aminov 2010), the first hospital use of an antimicrobial was actually by Emmerich and Löw in 1899. They attempted to utilize prepared extracts of *Pseudomonas aeruginosa,* which they dubbed Pyocyanase, to treat infections. However while the preparation did exhibit activity against numerous pathogenic bacteria, it was highly toxic to humans forcing the treatment to be abandoned (Emmerich and Löw, 1899). Unlike Emmerich and Löw, Ehrlich was successful in his pursuit of an antibiotic. In 1904 he utilized a large-scale screening program, a predecessor to today's high throughput screening techniques, to find a drug to treat syphilis, an endemic and nearly untreatable infection at the time. Ehrlich screened hundreds of organoarsenic derivatives of the toxic drug Atoxyl in rabbits before finding a compound that could cure syphilis-infected rabbits (Ehrlich and Hata, 1910). The compound 'Salvarsan', later replaced by the less toxic 'Neosalvarsan', became the most prescribed drug used to treat infections until its replacement by penicillin in the 1940s. This systematic screening approach championed by Ehrlich led to the discovery of thousands of compounds including sulfa drugs by Klarer, Mietzsch, and Domagk, derivatives of which are still viable therapeutics today.

However, of all these discoveries by far the most famous is the serendipitous discovery of penicillin by Alexander Fleming. For 12 years after his initial observation of a *Penicillium notatum* contaminant inhibiting the growth of *Staphylococcus* on a petri-plate Fleming tried to

solve the problem of purifying and stabilizing the active compound produced by the fungus but was ultimately unsuccessful. However in 1940 a team of researchers from Oxford succeeded and published a paper describing the purification of penicillin (Chain et al. 1940) which would lead to the mass production and distribution of penicillin in 1945.

The discovery of penicillin in combination with a more advanced version of Ehrlich's screening method developed by Selman Waksman in the 1940s, one that would later earn him a Nobel Prize, ushered in the golden age of antibiotic discovery during which almost all the antibiotic classes utilized today were discovered. Unfortunately, the golden age of antibiotics would end as quickly as it began. After roughly 20 years of success the well would run dry with fewer and fewer novel compounds being found.

Since the 1960s only 3 narrow-spectrum classes of antibiotics have been discovered and not a single new broad spectrum antibiotic class has been identified. Daptomycin, a lipopeptide active against Gram-positive cell membranes, was discovered in 1986 but wasn't approved for clinical use until 2003. The streptogramins, also specific to Gram-positives, were discovered in 1964 but similarly didn't make it to the clinic until 1998 (Lewis 2013). The latest antibiotics to make it to the clinic are the diarylquinolines which are only effective against *Mycobacterium tuberculosis*. However, resistance against diarylquinolines was reported six year before their first clinical use (Lewis 2013).

2.2.2 Rise of Antibiotic Resistance

Even before the widespread use of penicillin in the mid-1940s, there was concern in the scientific community regarding the possibility of pathogens gaining resistance to antibiotics (Abraham and Chain, 1940). However due to the long term use of arsenic based treatments for syphilis and little observed high level resistance to these treatments, the overall consensus was

that penicillin would likely follow the same trajectory (Rollo et al. 1952). Nevertheless while this remained largely true for *Treponema pallidum* (Cha et al. 2004), this was not the case for many clinically relevant pathogens especially among the Enterobacteriaceae. Initially the issue of resistance was moderated by the discovery of new compounds and synthetic derivatives of existing antibiotics outpacing the spread of resistance. Unfortunately, this trend did not last and as fewer and fewer compounds were being discovered the rate of resistance concurrently increased. Early antibiotics like the sulfa drugs and β-lactams enjoyed six and seven years of use respectively before widespread resistance was observed. Conversely newer drugs deployed near the tail end of the 1950s such as erythromycin, chloramphenicol, and vancomycin were only utilized clinically for one or two years before resistance was observed. This trend has worsened as resistance to newer drugs such as daptomycin, fidaxomicin, and bedaquiline had been reported before they are even approved for clinical use (Lewis 2013).

The consequence of the rise of resistance and lack of new antibiotics making it to market is the risk to human lives. It is estimated that 700,000 deaths occur world-wide due to antibiotic resistant infections, with 23,000 of those occurring in the United States, and 25,000 a year in Europe where advanced medical care is available (Aminov 2010, Watkins and Bonomo 2016, Jasovský et al. 2016). As resistance continues to rise and antibiotic development continues to flounder these numbers are projected to increase to 10 million deaths annually by 2050 with the economic cost associated with these infections estimated to reach US$100 trillion within that same time frame (O'Neill 2014). In light of these startling trends research into how resistance is acquired and regulated is sorely needed.

2.2.3 Mechanisms of Antibiotic Resistance

Three basic strategies can be used to describe the mechanisms that bacteria employ to avoid the action of antibiotics: (1) enzymatic degradation or modification of antibiotics, (2) modification of antibiotic targets, and (3) the combination of decreased membrane permeability and increased efflux.

Enzymatic degradation is a mechanism wherein the bacterium produces an enzyme to inactivate the offending antibiotic. Enzymatic degradation is most famously utilized by Gram-negative pathogens producing β-lactamases which degrade β-lactam antibiotics such as penicillin, and more recently extended spectrum β-lactamases and carbapenamases which confer resistance to the semi-synthetic derivatives of the original penicillin's such as methicillin and imipenem, a last resort antibiotic (Kumarasamy et al. 2010). Based on sequence homology studies all four classes of currently characterized β-lactamases have been identified in *A. baumannii* (Perez et al. 2007). Alternatively, if an antibiotic cannot be destroyed it can be modified to decrease efficiency of the drug. This is exemplified in *A. baumannii* by aminoglycoside-modifying enzymes. As the name suggests these enzymes inactivate aminoglycosides by modifying them via acetylation, adenylation, or phosphorylation. Clinical isolates have been identified carrying as many as 4 different aminoglycoside-modifying enzymes (Zhu et al. 2009).

The second mechanism is target modification. In this instance, the bacterium modifies the antibiotics target molecule so the antibiotic is no longer able to bind. This can be achieved through three distinct tactics, replacement of the target molecule with a different one that the antibiotic cannot bind, mutation of the target protein so the antibiotic binding site is removed, or post translational modification of the target site so the antibiotic can't bind (Lin and Lan 2014).

A. baumannii utilizes all of these target modification techniques to gain resistance to antibiotics. *A. baumannii* has been shown to replace its normal penicillin binding proteins with ones that have a low binding affinity for imipenem which confers resistance by replacement (Gehrlein et al. 1991). Mutations in the DNA gyrase and topoisomerase IV genes *gyrA* and *parC* provide resistance to quinolones by removal of the quinolone binding site (Vila et al. 1995, Higgins et al. 2004). Strains of *A. baumannii* have been identified that carry the *tetM* gene which encodes a protein that protects the ribosome from the action of tetracycline (Ribera et al. 2003).

The third mechanism of resistance utilized by bacteria is a two-part mechanism based on a combination of decreased uptake and increased efflux of antibiotics. *A. baumannii* utilizes both branches of this mechanism to gain resistance to antibiotics. Decreased expression of a variety of outer membrane porins including the 22, 33, 37, and 44 kDa outer membrane porins have been linked to carbapenem resistance (Bou et al. 2000, Quale et al. 2003, Tomas et al. 2005, Catel-Ferreira et al. 2011). Loss of lipopolysaccharide from the outer membrane of *A. baumannii* and the resulting membrane destabilization have been shown to provide colistin resistance (Moffatt et al. 2010), and disruption of the *ompA* gene can provide decreased susceptibility to chloramphenicol, aztreonam, and nalidixic acid (Smani et al. 2014). *A. baumannii* has four different types of efflux pump available to it which contribute to antibiotic resistance. These include the major facilitator superfamily (MFS), multidrug and toxic compound extrusion (MATE), small multidrug resistance (SMR), and resistance nodulation division (RND) superfamily. Of these 4 efflux pump families the RND and MFS are most commonly linked to clinical level resistance, conferring intrinsic resistance to multiple classes of antibiotics including last resort antibiotics such as the fluoroquinolones, carbapenems, and tigecycline (Ruzin et al. 2007, Damier-Piolle et al. 2008a, Hou et al. 2012).

2.3 Resistance Nodulation Division Efflux Pumps

Of the energy dependent efflux pumps found in *A. baumannii*, the primarily mediator of resistance are the RND efflux pumps. These tripartite pumps provide intrinsic resistance to a wide variety of antimicrobials. To date, three RND pumps have been described in *A. baumannii*, AdeABC (Magnet et al. 2001), AdeFGH (Coyne et al. 2010), and AdeIJK (Damier-Piolle et al. 2008a).

AdeABC was the first RND efflux pump to be characterized in *A. baumannii*, and of the three, plays the largest role in the multi-drug resistant phenotype characteristic of *A. baumannii* isolates (Marchand et al. 2004, Yoon et al. 2013). AdeABC contributes to resistance to aminoglycosides and tigecycline, as well as other non-fluoroquinolone antibiotics including carbapenems (Magnet et al. 2001, Higgins et al. 2004, Ruzin et al. 2007). While AdeFGH and AdeIJK do not contribute as much to multi-drug resistance as AdeABC, they have been shown to combine to provide synergistic resistance to tigecycline (Damier-Piolle et al. 2008a).

Among the three RND pumps in *A. baumannii*, the AdeIJK efflux pump is of particular interest for two reasons. Firstly, AdeIJK has been reported in all strains of *A. baumannii* and, as opposed to the AdeABC and AdeFGH pumps, is constitutively expressed (Rosenfeld et al. 2012), thus suggesting that AdeIJK may play an important physiological role for the organism. Secondly, unlike other RND pump-encoding operons, *adeIJK* does not have a linked regulator gene, instead its expression appears to be solely regulated by a TetR-type transcriptional repressor AdeN located 813 kb upstream of the *adeIJK* operon (Rosenfeld et al. 2012). RND-efflux pumps in other organism have been shown to be controlled by regulators that are not directly linked to the pump operon; however, in these cases the regulator often functions as a

global transcription regulator which controls a much larger subset of genes and can be involved in a wide variety of cellular functions (Kumar and Schweizer 2005).

2.4 TetR Transcriptional regulators

TetR transcription regulators are a large diverse group of transcription regulators named for the TetR protein that is responsible for regulation of tetracycline resistance in *E. coli* (Beck et al. 1982). Since then more than 2400 TetR transcription regulators have been identified of which nearly 25% play a role in antibiotic resistance (Ahn et al. 2012). However, while the TetR protein is both the namesake and model for the group, it does not accurately represent the diversity within the TetR family. TetR proteins have been shown to act as both activators and repressors, serve as local or global regulators, can be autoregulatory or under the control of other regulators, and can interact with small molecules or proteins (Yu et al. 2010). Despite the significant diversity in TetR regulators there are some general trends that can be applied to most members of the group.

The majority of TetR proteins act as transcriptional repressors of divergently encoded genes generally within ~200bp of where the regulator is encoded. TetR regulators largely function as dimers binding to palindromic operator sequences with an N-terminal DNA binding domain and a C-terminal inducer ligand binding domain. Although the binding partners of most TetR regulators are unknown those that have been identified once again suggest a significant diversity of binding partners including antibiotics, bile salts, fatty acids, and metal ions (Cuthbertson and Nodwell 2013). Despite the wide variety of possible ligand binding partners available those that have been characterized so far suggest that ligand binding results in an increased separation of the two DNA-binding domains preventing them from fitting into adjacent major grooves of the DNA double helix (Reichheld et al. 2009).

2.5 Previous Work

Previous work in our laboratory, involved characterization of a spontaneous mutant of ATCC17978 generated by exposing it to increasing concentrations of triclosan, a biocide used in many commercial products. This strain, AB042, contained a 73bp deletion in *adeN* which resulted in overexpression of the AdeIJK RND efflux pump. Regulatory role of *adeN* with respect to AdeIJK was confirmed by complementing AB042 with the wild-type *adeN* (Fernando et al. 2014). However, interestingly, transcriptomic and proteomic analysis of AB042 revealed significant changes in the expression of various other genes (Fernando et al. 2017). This, in combination with its atypical genetic structure led to the hypothesis that AdeN may be playing a role as a global transcription regulator in *Acinetobacter baumannii*. However, since AB042 also contains point mutations in *fabI* and *fabB*, genes that encode two enzymes involved in fatty acid biosynthesis that when mutated confer resistance to triclosan, we were unable to directly attribute any of the changes in gene expression and the corresponding phenotypes to the activity of AdeN.

2.6 Hypothesis and Research Objectives

My working hypothesis is that AdeN acts as a global transcription regulator that controls resistance and virulence in *A. baumannii*.

As such this hypothesis was tested through the following objectives;

(1) To create deletion mutants of *adeN, adeIJK,* and a double mutant in ATCC17978

(2) Use a multi-omics approach to elucidate a putative AdeN regulon

(3) Characterize the phenotypic effect of *adeN* and *adeIJK* deletion on virulence and resistance associated phenotypes.

A secondary objective for my graduate work was to create fluorescent tagging plasmids optimized for expression in *A. baumannii* using the miniTn*7* single copy insertion system

described by Kumar *et al*. 2010. Four constructs were designed to constitutively express four different fluorescent genes, green fluorescent protein (GFP), yellow fluorescent protein (YFP), cyan fluorescent protein (CFP), and *Discosoma* sp. red fluorescent protein (DsRed). These constructs could be used in virulence and competition assays and for any fluorescent imaging experiments.

Thus my secondary research objective was;

(1) To create four plasmid constructs for single copy insertion of fluorescent genes that would be constitutively expressed in *A. baumannii.*

3 Materials and Methods

3.1 Bacterial Strains, Plasmids, and Oligonucleotides

All the bacterial strains and their characteristics are described in Table 1. All primers used in this study are detailed in Table 2.

Table 1: All bacterial strains and plasmids used in this study.

Strain or Plasmid	Characteristics	Reference or Source
A. baumannii ATCC17978	Wild-type	ATCC
A. baumannii AB119	ATCC17978 *adeN*::Gm	This Study
A. baumannii AB141	ATCC17978 Δ*adeN*	This Study
A. baumannii AB183	AB141::*adeN*	This Study
A. baumannii AB181	ATCC17978 *adeIJK*::Gm	This Study
A. baumannii AB185	ATCC17978 Δ*adeIJK*	This Study
A. baumannii AB182	AB141 *adeIJK*::Gm	This Study
A. baumannii AB186	AB141 Δ*adeIJK*	This Study
A. baumannii	miniTn*7*-GFP insertion into ATCC17978	This Study
A. baumannii	miniTn*7*-YFP insertion into ATCC17978	This Study
A. baumannii	miniTn*7*-CFP insertion into ATCC17978	This Study
A. baumannii	miniTn*7*-DsRed insertion into ATCC17978	This Study
E. coli DH5α	F- endA1 glnV44 thi-1 recA1 relA1 gyrA96 deoR nupG Φ80dlacZΔM15 Δ(lacZYA-argF)U169, hsdR17(rK- mK+), λ–	Laboratory collection
E. coli SM10	KmR, thi-1, thr, leu, tonA, lacY, supE, recA::RP4-2-Tc::Mu, pir	Laboratory collection
pMO130	Suicide vector, Km^r	(Hamad et al. 2009)
pUC18T-miniTn*7*-Gm-LAC	Single copy insertion vector, Gm^r, Amp^r	(Choi et al. 2005)
pPLS168	pMO130-*adeN*GmFRT, *adeN* knockout suicide vector, Gm^r, Km^r	This Study
pPLS178	pMO130-*adeIJK*GmFRT, *adeIJK* knockout suicide vector, Gm^r, Km^r	This Study
pFLP2	Plasmid expressing Flp-recombinase, Amp^r	(Choi and Schweizer 2005)

pTNS2	Plasmid expressing transposon insertion machinery,	(Choi et al. 2005)
pPLS223	pUC18T-miniTn*7*-Gm-LAC-*adeN*, *adeN* single copy insertion complementation vector, Gm^r, Amp^r	This Study
DQ493881	pUC18T-miniTn*7*-Tmp-GFP, Tmp^r, Amp^r	(Choi and Schweizer 2006)
DQ493884	pUC18T-miniTn*7*-Tmp-DsRed, Tmp^r, Amp^r	(Choi and Schweizer 2006)
DQ493883	pUC18T-miniTn*7*-Tmp-YFP, Tmp^r, Amp^r	(Choi and Schweizer 2006)
DQ493882	pUC18T-miniTn*7*-Tmp-CFP, Tmp^r, Amp^r	(Choi and Schweizer 2006)
pPLS228	pUC18T-miniTn*7*-Gm-*tac*, Gm^r, Amp^r	This Study
pPLS236	pUC18T-miniTn*7*-Gm-*tac*-GFP, single copy insertion of GFP, Gm^r, Amp^r	This Study
pPLS237	pUC18T-miniTn*7*-Gm-*tac*-CFP, single copy insertion of CFP, Gm^r, Amp^r	This Study
pPLS238	pUC18T-miniTn*7*-Gm-*tac*-YFP, single copy insertion of YFP, Gm^r, Amp^r	This Study
pPLS239	pUC18T-miniTn*7*-Gm-*tac*-DsRed single copy insertion of DsRed, Gm^r, Amp^r	This Study

Table 2: All Primers used in this study

Primer	Sequence	Purpose	Source or Reference
AdeN-Upstream-Fwd	TTG ATG TTC GAA TCG TGG CGG CAA CC	Amplification of 1kb fragment upstream of *adeN*. Reverse primer contains 23bp sequence similarity to the Gm^r-cassette, indicated by underlined bases.	This Study
AdeN-Upstream-Rev	AGA GCG CTT TTG AAG CTA ATT CGT CAT AAA ATT TAA TAA CGA CGG CTA A		
Gm-Fwd	CGA ATT AGC TTC AAA AGC GCT CTG A	Amplification of Gm^r -cassette	This Study
Gm-Rev	CGA ATT GGG GAT CTT GAA GTT CCT		
AdeN-Downstream-Fwd	AGG AAC TTC AAG ATC CCC AAT TCG TAA TT TTT TGC ATT TTG AAA TGC TT	Amplification of 1kb fragment downstream of *adeN*. Forward primer contains 24bp sequence similarity to the Gm^r-cassette, indicated by underlined bases	This Study
AdeN-Downstream-Rev	GCT TCT GTT CTT CTT CTT GTC CCA TGC TTG C		
AdeN-FL-Fwd	GAT AAG CAG TGT TAG CCG TCG	*adeN* Screening Primer; 1131bp marked deletion; 725bp Wild-type;	(Fernando et al. 2014)
AdeN-FL-Fwd	AGT CTA CTA TAC TAT AAG CAT TTC		
AdeN-FL-Fwd-PstI	ATA CTG CAG ATA AGC AGT GTT AGC CGT CG	Amplification of full length *adeN* with *Pst*I and *Hind*III restriction sites for cloning into pUC18T-miniTn*7*-Gm-LAC. Restriction sites underlined	This Study
AdeN-FL-Rev-HindIII	AAT AAG CTT AGT CTA CTA TAC TAT AAG CAT TTC		
GlmS_Fwd	TTT GCT GAT GAA AAT AGC GG	Primers for confirmation of miniTn*7* insertion downstream of *glmS2*	(Kumar et al. 2010)
Tn*7*R_Rev	CAC AGC ATA ACT GGA CTG ATT TC		
AdeN-Seq-Fwd	AAG AGC TGG GCA TGG ACT CT	Primers used to confirm *adeN* deletion by sequencing	This Study
AdeN-Seq-Rev	GAA ATA CGA GTG CGT GTG CT		
AdeIJK-Upstream-Fwd	GTC GAG TTC GCT TTG AAC AAT GGA AG	Amplification of 1kb fragment upstream of *adeIJK*. Reverse primer contains 25bp sequence similarity to the Gm^r-cassette, indicated by underlined bases.	This Study
AdeIJK-Upstream-Rev	TCA GAG CGC TTT TGA AGC TAA TTC GTC TGG TGC CCA AAG CTT AGC CGA CAT		

AdeIJK-Downstream-Fwd	AGG AAC TTC AAG ATC CCC AAT TCG ATC TAG TGC TGA ACT TAA AAA GCA A	Amplification of 1kb fragment downstream of *adeIJK*. Forward primer contains 24bp sequence similarity to the Gm^r-cassette, indicated by underlined bases	This Study
AdeIJK-Downstream-Rev	AAA CAA CAG GGC ATA TGG AAA ATT A		
AdeIJK-FL-Fwd	ACC CGT AAG TTC ACC ACC	*adeIJK* screening primer; 743bp unmarked deletion; 6238bp Wild-type	This Study
AdeIJK-FL-Rev	ACT GCT TTG GCT CTG GTT		
AdeJ-Int-Fwd	TGT AGG TCA GTT AGG TGG TGC	*adeJ* internal screening primer; 1003bp Wild-type; absent in deletion	This Study
AdeJ-Int-Rev	AAC AGC ATA GAG CAC GCC AG		
16S-RT-Fwd	CTT CGG ACC TTG CGC TAA TA	qRT PCR primer for the 16S rRNA housekeeping gene	(Fernando et al. 2014)
16S-RT-Rev	ATC CTC TCA GAC CCG CTA CA		
AdeI-RT-Fwd	GCA GCA GCT AAG GCT CAA GT	qRT PCR primer for *adeI* the gene encoding the transmembrane domain of the AdeIJK RND efflux pump	This Study
AdeI-RT-Rev	TGC AGT AAC CAA AGC ACC AG		
AdeJ-RT-Fwd	TTC AGC GTG GTA TGG CAT TA	qRT PCR primer for *adeJ* the efflux pump gene of the AdeIJK RND efflux pump	This Study
AdeJ-RT-Rev	AAT CCG GCA GTT ACA CCA AG		
AdeK-RT-Fwd	GCG TTT GCT TGA AGT GAT TG	qRT PCR primer for *adeK* the outer membrane porin gene of the AdeIJK RND efflux pump	This Study
AdeK-RT-Rev	TGG AAG CTG GTT GTT CTG TG		
FP_Fwd_XhoI	AGG AAT TCC TCG AGA AGC TTG G	Cloning Primers for insertion of Fluorescent genes into pUC18T-miniTn*7*-Gm-*tac*. Forward primer used for all reactions. GFP primer used to amplify GFP, YCR primer used to amplify YFP, CFP, and DsRed. Restriction sites underlined	This Study
GFP_Rev_SacI	TTA GAG CTC TCT AGA ATT AAA GAG GAG AAA TTA AGC		
YCR_Rev_SacI	TTA GAG CTC CAC ACA TCT AGA ATT AAA GAG GAG		
LacIq_Fwd	TCA CTG CCC GCT TTC CAG	Screening primer for identifying loss of *lacIq* in pUC18T-miniTn*7*-Gm-*tac*. 925bp intact, 237bp truncated	This Study
LacIq_Rev	ACA ACA ACT GGC GGG CAA AC		

3.2 Media and Growth Conditions

All strains were grown in Lennox LB (Difco Laboratories, Mississauga, ON, Canada) at 37°C with shaking at 200 rpm unless otherwise stated.

3.3 Genomic and Plasmid DNA Extractions

Genomic extractions were performed using the MoBio UltraClean Microbial DNA Isolation Kit (MoBio, Carlsbad, CA, USA) following the manufacturer's instructions. Plasmid DNA extractions were performed using the BioBasic Plasmid DNA Mini Preps kit (BioBasic, Markham, ON, Canada) following the manufacturer's instructions.

3.4 Gel Extraction

DNA gel extractions were performed using the Thermo Scientific GeneJet Gel Extraction Kit (Thermo Fisher Scientific, Toronto, ON, Canada) following the manufacturer's instructions.

3.5 DNA manipulations

3.5.1 Polymerase Chain Reaction (PCR)

PCR for screening and amplification was performed using the BioRad T100 Thermal Cycler (Bio-Rad Laboratories, Mississauga, ON, Canada). General cycling conditions are as follows, initial and cycle denaturation both occurred at 95°C, for 3 minutes and 30 seconds respectively. Annealing temperatures for each primer set were calculated by averaging the annealing temperature of each primer and then subtracting 4°C. Extension was performed at 72°C for 1 minute per kb of DNA amplified. The cycle would repeat for 34 cycles before a final 5 minute extension at 72°C. General PCR was performed with Taq polymerase (FroggaBio, North York, ON, Canada), using the buffers provided with the polymerase. dNTPs (FroggaBio) were used at a concentration of 100μM. Primers were all purchased from IDT (Integrated DNA

Technologies, Toronto, ON, Canada) and diluted to 9μM for all PCRs. PCR reactions to screen for recombinant plasmids were routinely performed in 10μL volume which were made up as follows. 0.1μL dNTPs, 0.1μL of forward and reverse primers, 1μL 10X buffer, 0.1μL Taq polymerase, 0.1μL template, 7.6μL water. Reactions were scaled up appropriately when needed. Genomic or plasmid DNA was used as the template. Occasionally, template was also prepared by boiling a small amount of cells resuspended in 50μL of water for 10 minutes and using the supernatant for PCR reaction.

3.5.2 Restriction Digestion and Ligation

All restriction digestion reactions were performed using enzymes from NEB (New England Biolabs, Whitby, ON, Canada) with the provided buffers. Restriction digestion conditions for cloning purposes were as follows, 2.5μL of the appropriate buffer, 1 unit of restriction enzyme, up to 1μg purified DNA, and then made up to 25μL total volume with water. Restrictions were incubated at 37°C for 90 – 120 minutes. Restriction digestion for confirming plasmid constructs were scaled down to 10μL and incubated for 60 minutes.

Ligations were performed using T4 DNA Ligase (Thermo Fisher Scientific, Waltham, MA, USA) using the manufacturers recommended reaction conditions scaled down to 10μL reactions. Sticky ended ligations were performed using a 3:1 or 5:1 insert to vector ratio while blunt ended ligations were performed using a 6:1 or 10:1 insert to vector ratio. All ligation ratios were normalized by fragment size using the following calculation;

$$ng\ vector \times \frac{size\ of\ insert\ (bp)}{size\ of\ vector\ (bp)} \times ratio = ng\ insert$$

In all ligations used 50ng of digested vector and were incubated at 16°C overnight in a thermocooler.

3.5.3 Splice-overlap-extension PCR (SOEing)

Splice overlap extension polymerase chain reaction was utilized to construct the gene knockout cassettes for deletion of genes. The method used to create the constructs was based on a previously published method (Choi and Schweizer 2005) with the following modifications. The basic strategy in SOEing PCR requires two separate sets of PCR reactions to link three distinct PCR products together into a single fragment.

In the first PCR two sets of gene specific primers are used to amplify ~1kb fragments flanking the gene of interest including 5-15bp of the start and end of the target gene, these will constitute the two external fragments of the SOEing product hereafter referred to as the upstream and downstream fragments. The third internal fragment is a gentamicin resistance cassette flanked by *FRT* sites which is amplified from a pMO130 vector. The three separate fragments were amplified with Q5 High-Fidelity DNA polymerase (New England Biolabs) and gel purified.

The second PCR utilizes 23-24bp of complimentary sequence designed into the reverse primer of the upstream fragment and the forward primer of the downstream fragments, to the FRT sites located at each end of the internal fragment. The completed cassette was assembled by mixing 50ng of each purified fragment in a Q5 High-Fidelity DNA polymerase PCR reaction without primers. The reaction was initially cycled five times (Tm=55°C) during which the complementary sequence between the upstream and downstream fragments with the internal fragment mentioned above can anneal and extension occurs from these annealed regions filling in the complete fragment. After the first five cycles the upstream fragments forward primer and the downstream fragments reverse primer were added and the PCR cycle was allowed to

continue for another 34 cycles wherein the assembled 3kb fragment is amplified. The resultant 3kb product was gel purified before cloning into the pMO130 suicide vector.

3.6 Preparation of Competent Cells

3.6.1 Chemically Competent *E. coli*

Overnight cultures of *E. coli* were subcultured (1:100 v/v dilution) into 125mL of fresh LB broth and allowed to grow to an OD_{600} = 0.4-0.6. Cultures were pelleted by centrifugation at 5000rpm for 5 minutes at 4°C. While maintaining cells on ice supernatants were decanted before resuspending in 40% of the original culture volume of ice-cold TFB1 buffer (100mM Rubidium Chloride, 50mM Manganese Chloride, 30mM Potassium Acetate, 10mM Calcium Chloride, 15% Glycerol, pH5.8). Cells were pooled and incubated on ice for 5 minutes before pelleting by centrifugation at 5000 rpm for 5 minutes at 4°C. Supernatants were again removed before cells were resuspended in 4% of the original culture volume of ice-cold TFB2 buffer (10mM MOPS, 10mM Rubidium Chloride, 75mM Calcium Chloride, 15% Glycerol, pH 6.5). Resuspended cells were incubated on ice for 30-60 minutes before flash freezing in dry ice and ethanol.

3.6.2 Electrocompetent *A. baumannii*

Four aliquots of 1.5 mL overnight cultures of *A. baumannii* were pelleted at 12000 rpm for 2 minutes. Culture supernatants were removed from the cell pellet and discarded. Cell pellets were then washed three times with sterile ice cold water with pelleting at 12000 rpm for 2 minutes between washes. Washed cells were then pooled together and made up to a final volume of 150µL with sterile ice cold water. Cells prepared by this method were used immediately.

3.7 Transformation of Competent Cells

3.7.1 Chemical Transformation

Chemical transformations of *E. coli* were performed using the heat shock method (Dale and Greenaway 1984). Briefly 5µL of ligation mixture was incubated on ice with 50µL chemically competent cells for 30 minutes. Transformation mixtures were then heat shocked at 42°C for 45 seconds and then allowed to rest for 5 minutes on ice before recovery in Super Optimal Broth (SOC) (Oxoid Inc., Nepean, ON, Canada) for 1 hour at 37°C. After recovery cells were pelleted at 12000 rpm for 2 minutes and resuspended in 100µL of SOC broth before plating the transformed cells on appropriate plates.

3.7.2 Electroporation

Electroporation reactions were performed by mixing 50µL of prepared competent cells with 100 – 200ng of purified plasmid up to a maximum of 5µL total volume added. When multiple plasmids were electroporated at the same time equal amounts of plasmid were used again up to a maximum of 5µL added volume. Electroporation mixtures were allowed to rest on ice for 10 minutes before transfer to electroporation cuvettes (Thermo Fisher Scientific). All electroporation reactions were performed in 2mm cuvettes which were stored at -20°C until use. After transfer to the electroporation cuvette cells were charged at 1.7kV in an Eppendorf Electroporator 2510 (Eppendorf, Mississauga, ON, Canada) and 1mL of prewarmed SOC broth was immediately added following charge. Cells were transferred to a 13mL culture tube and allowed to recover at 37°C for 1 – 4 hours. After recovery 100µL of the recovery culture was spread plated on appropriate growth media. The remaining recovery culture was pelleted at 12000 rpm for 2 minutes and resuspended in 100µL before plating the remaining cells.

3.8 Gene Deletions in *Acinetobacter baumannii*

3.8.1 Conjugation

Conjugations were performed using a previously described method (Mohammad et al. 2013). Briefly 200μL of overnight cultures of the strains to be mated were mixed together in 1.1mL of fresh LB broth. Mixed cultures were spun down at 1200 rpm for 2 minutes and the cell pellets were washed 3 times in 1mL of fresh LB broth. After washing, the mixed cell pellets were resuspended in 10μL of LB broth and slowly spotted onto a 3cm x 3cm piece of nitrocellulose placed on a pre-warmed LB agar plate. After spots had dried they were incubated at 30°C overnight. Following overnight incubation conjugation mixtures were collected by soaking the nitrocellulose in 500μL 0.85% sterile saline for 10 minutes. The conjugation mixture was then washed 3 times in 1 mL 0.85% saline before plating on Simmons Citrate agar (Sigma Aldrich, Oakville, ON, Canada), a selective media for *A. baumannii* which can use citrate as a carbon source, supplemented with 50μg/mL kanamycin (Bioshop Canada Inc., Burlington, ON, Canada) and allowed to incubate at 37°C for 48 hours. After incubation, conjugates were screened by plating on kanamycin 50 μg/mL LB agar and gentamicin (BioBasic, Markham, ON, Canada) 50μg/mL LB agar. Recombination of the plasmid would be indicated by resistance to both kanamycin and gentamicin.

3.8.2 Homologous Recombination

To select for the second recombination event, which would result in the marked deletion mutant, the *sacB* gene present on the pMO130 backbone was utilized. *sacB* encodes an enzyme from *B. subtilis* called levansucrase which converts sucrose into levans, a lethal compound for bacteria. Merodiploid colonies were streaked onto Vogel-Bonner minimal medium (VBMM) agar (Schweizer 1991) supplemented with 5% sucrose (BioBasic) and 30μg/mL gentamicin and

incubated at 30°C for 48 hours. Colonies from these plates were patched on gentamicin 50μg/mL LB agar and kanamycin 50μg/mL LB agar. Colonies that exhibited resistance to gentamicin and susceptibility to kanamycin had undergone the second recombination event resulting in a marked deletion of the target gene. Marked deletions were confirmed by PCR with AdeN_FL_Fwd and AdeN_FL_Rev primers.

3.8.3 Excision of Gentamicin marker

Excision of the gentamicin marker was completed by use of the pFLP2 plasmid which encodes a flip-recombinase which recognizes the FRT sites flanking the gentamicin cassette and inducing a recombination event wherein the gentamicin cassette is removed leaving behind a single FRT site (Hoang et al. 1998). pFLP2 was introduced into the marked deletion strains via electroporation as described above and plated onto LB agar plates supplemented with 200μg/mL carbenicillin (Duchefa Biochemie, Haarlem, Netherlands). Following overnight incubation at 37°C colonies were patched on carbenicillin 200μg/mL LB agar and gentamicin 50μg/mL LB agar to screen for susceptibility to gentamicin. Excision of the gentamicin cassette was confirmed by PCR before unmarked deletion mutants were streaked onto LB agar with 5% sucrose to cure the pFLP2 plasmid which also carries a *sacB* gene. Colonies cured of the pFLP2 plasmid exhibited susceptibility to carbenicillin when patched on LB agar and carbenicillin 200μg/mL LB agar. Unmarked deletion mutants were confirmed by Sanger sequencing across the deletion scar at the sequencing facility of Genome Quebec (Montreal, QC, Canada) using AdeN_Seq_Fwd and AdeN_Seq_Rev primers.

3.9 Complementation of Gene Deletions

3.9.1 Chromosomal Complementation

adeN was inserted in single copy in the chromosome of *adeN* deletion mutant AB141 by the use of the miniTn*7* system (Choi and Schweizer 2006). *adeN* was cloned into the pUC18-miniTn*7*-Gm-LAC plasmid which utilizes the *lacI*^{q} repressor system and a P*tac* promoter allowing for IPTG induction of *adeN* expression. The resultant plasmid pPLS223 was electroporated into AB141 with the pTNS2 plasmid which contains genes encoding enzymes necessary to insert the transposon into the target chromosome (Choi and Schweizer 2006). Following electroporation cells were plated on gentamicin 50μg/mL LB agar and screened for insertion of the *adeN* gene downstream of *glmS2* via PCR with AdeN_FL primers and Tn*7*R_GlmS primers.

3.10 Quantitative Reverse Transcriptase PCR

3.10.1 RNA extraction, DNase Treatment, and cDNA synthesis

Before RNA extraction cells were prepared by subculturing 30μL of overnight culture into 3mL of fresh LB broth and monitoring growth to an OD_{600} of 0.6 – 0.7. Once cultures had reached the desired OD_{600} cells were spun down and the supernatant removed. Dry pellets were then frozen overnight at -70°C before RNA extraction. RNA extractions were performed using the Qiagen RNeasy Mini kit (Qiagen, Toronto, ON, Canada) following the manufacturers instructions. Extracted RNA was diluted to 200ng/μL in RNase free water before DNase treatment was performed on a total of 1μg RNA using the Qiagen RNase free DNase Set (Qiagen) following the manufacturer's instructions. Synthesis of complimentary DNA (cDNA)

was completed with the Invitrogen Superscript VILO cDNA synthesis kit (Invitrogen, Burlington, ON, Canada) following the manufacturer's instructions.

3.10.2 Quantitative reverse transcriptase PCR

qRT-PCR was performed with the Applied Biosystems SYBR-Select Master Mix (Applied Biosystems Inc., Foster City, CA, USA) on a StepOne-Pus Real Time PCR platform (Applied Biosystems Inc.). All real time PCR primers were designed using the Invitrogen OligoPerfect tool. To ensure there was no genomic contamination of cDNA samples DNase treated RNA was used as a negative control for all primer sets in addition to a No-Template-Control which substituted water for cDNA. Relative expression was calculated using 16S rRNA as the reference gene by Pfaffl method (Pfaffl 2001).

3.11 Phenotypic Testing

3.11.1 Growth Curves

Overnight cultures of bacterial cells were subcultured into fresh LB broth and allowed to grow to an OD_{600} of 0.6 before a 10% inoculum of these cells were again subcultured into the desired medium. 125µL of each diluted culture was then distributed into 3 wells of a round bottom 96 well polystyrene microtitre plate (Sarstedt, Montreal, QC, Canada). Plates were then incubated at 37°C in a SpectraMax M2 plate reader (Molecular Devices Sunnyvale, CA, USA) with 30 seconds of shaking at 200 rpm before each reading which occurred every thirty minutes. Two biological replicates were used for all strains.

3.11.2 Antibiotic Susceptibility Testing

Antibiotic susceptibility testing was performed by the broth microdilution method described by the Clinical and Laboratory Standards Institute on at least two biological replicates

(Clinical and Laboratory Standards Institute 2012). Results were expressed as the Minimum Inhibitory Concentration (MIC) of the antibiotic that inhibited visible growth of the culture given in μg/mL.

3.11.3 Biofilm Assays

Biofilm assays were performed as previously described (Iwashkiw et al. 2012) with the following modifications. Overnight cultures were subcultured and grown to an OD_{600} of 0.5 before 1:100 dilution in Mueller Hinton Broth (Sigma Aldrich, Oakville, ON, Canada). 125μL of diluted cultures were distributed into at least six wells of a 96-well polystyrene, round-bottom microtiter plate (Sarstedt) before stationary incubation at 37°C for 48 hr. Cultures were removed by washing twice with MilliQ water. Biofilms were stained with 150μL of 0.5% w/v crystal violet (Thermo Fisher Scientific) in ethanol (95%) and incubated with gentle shaking for 30 minutes. Crystal violet was washed out of the wells by gently submerging in MilliQ water 3-4 times. Plates were then air dried for at least four hours, before crystal violet was extracted with 150 μL 2% SDS by incubating at room temperature with gentle shaking for 30 minutes. Following extraction, the solution was transferred to a fresh 96-well plate and absorbance was measured at 580 nm using a SpectraMax M2 plate reader (Molecular Devices).

3.11.4 Motility

Motility assays were performed in semi-solid agar (0.3% agar) with overnight cultures that had been normalized to an OD_{600} of 1 in LB broth. 3μL of normalized cultures were stab inoculated into the center of the semi-solid agar plates and allowed to dry for 15 minutes before overnight incubation at 37°C. Motility was then evaluated by measuring the maximum distance travelled from the inoculation point in two different directions and combining the measures. Assays were performed using 3 biological replicates and at least 4 technical replicates.

3.11.5 Virulence assays with *Galleria mellonella*

Virulence assays were carried out following a previously published method (Gaddy et al. 2012). Briefly, overnight cultures were normalized to a 0.5 McFarland Standard in Phosphate buffered saline (PBS) resulting in an inoculum containing 1.5 x 10^8 cfu/mL which was confirmed by plate count methods. Larvae were prepared for injection by cleaning the abdominal side with a cotton-tipped applicator soaked in 70% ethanol. Before injection with 10μL of inoculum into the second pro-leg, larvae were briefly chilled on an icepack to minimize movement. A separate set of ten worms were injected with 10μL of PBS to serve as a negative control. After injection larvae were placed in petri-plates lined with filter paper and incubated at 37°C. Larvae were monitored every hour for 24 hours. Survival curves and statistical analysis were generated using GraphPad Prism (GraphPad Software Inc., La Jolla, CA, USA).

3.12 Fatty Acid Extraction

Fatty Acid extraction and analysis was performed as outlined below. Two biological replicates of each strain were grown overnight in 100mL of LB medium at 37 °C with shaking at 200 rpm for 16-18 hours. Cultures were pelleted at 5000 xg for 15 minutes. Cells were then washed twice in PBS and resuspended in 1mL of water. Resuspended cells were transferred to a clean 15mL screw-cap centrifuge tube and 10mL of 2:1 chloroform: methanol and 2mL of water was added to the cell suspension. Cell suspensions were homogenized by shaking and vortexing for 30 seconds. Homogenized cell suspensions were centrifuged for 12 minutes at 2000 rpm before incubating at 4°C overnight to allow for phase separation. The following morning the bottom organic phase was collected and transferred to a clean 15mL screw-cap centrifuge tube

and dried off in a nitrogen evaporator at 45°C until no solvent remained. 6mL of chloroform was added to the remaining extraction mixture and homogenized by shaking and vortexing for 30 seconds followed by centrifugation at 2000 rpm for 12 minutes. After centrifugation, the organic layer was collected and added to the 15mL tube containing the previously extracted and dried fatty acids before drying in a nitrogen evaporator at 45°C. After drying fatty acids were transferred to a clean 5mL screw-cap tube by rinsing twice with 1mL hexane and then dried under nitrogen. Fatty acids were methylated by solubilizing fatty acids in 1mL toluene by vortexing for 10 seconds before adding 1.2 mL of 3N methanolic HCl and incubating at 80°C for 1 hour. After allowing to cool, suspension was transferred to a fresh 15mL screw-cap tube and 1mL of water and 1mL of hexane were added. Mixtures were vortexed briefly before centrifuging at 2000 rpm for 4 minutes. The organic phase containing methylated fatty acids (top) was collected and transferred to a clean 8mL tube and dried in a nitrogen evaporator at 45°C. Hexane and water extraction was repeated and all collected methylated fatty acid suspension was dried under nitrogen at 45°C. Fatty acids were then resuspended in 1mL of hexane and transferred to gas chromatography vials and sent to the Department of Human Nutritional Sciences, Analytical Laboratory at the University of Manitoba for GC analysis using a 100m DB-225 column. Fatty Acid percentages were calculated by comparing the area under to curve of each fatty acid to an internal reference.

3.13 Scanning Electron Microscopy

Overnight cultures of bacteria were diluted 1:100 in LB broth and grown to an $OD_{600} = 0.8$. Cells were then washed twice in ice cold water before diluting to an $OD_{600} = 0.01$ in ice-cold water and spotting onto the sample stud. Samples were allowed to air dry overnight before

imaging on a Hitachi TM-1000 Scanning Electron Microscope (Hitachi Canada, Mississauga, ON, Canada).

3.14 RNA-Seq Sample Preparation and Analysis

Total cellular RNA was extracted as described above using the Qiagen RNeasy Mini kit (Qiagen). RNA-Sequencing was performed on two biological replicates of ATCC 17978, and AB141 at the Children's Hospital Research Institute of Manitoba (CHRIM). Enrichment and sequencing was performed using the Illumina MiSeq Platform (Illumina, Victoria, BC, Canada). Analysis of the sequencing data was performed using Galaxy online analysis kit version 2.2.6.2 (Afgan et al. 2016). Raw read (151bp paired end reads) quality was analyzed with FastQC and reads with a Phred score >30 were selected for further analysis. Adapter sequences were removed using Trim Galore! (ver. 0.4.1) and sequences were aligned to the genome with Bowtie2 (Langmead and Salzberg 2012). Relative expression and statistical analyses were performed using the Cufflinks pipeline (Trapnell et al. 2010). RNA-Seq data has been deposited to GenBank under the accession number GSE89504.

3.15 Proteomics Sample Preparation and Analysis

Five mL of overnight cultures were used to inoculate 500mL LB broth and grown to an A_{600} ≅ 0.8. Cells were harvested at 10000 xg for 10 minutes at 4°C, and washed in 10% glycerol. Cell pellets were frozen at -70°C until protein was extracted. Further processing, mass spectrometry, and analysis was performed at the National Microbiology Laboratory (NML, Winnipeg, Manitoba) in the Mass Spectrometry and Proteomics Core Facility. Thawed cell pellets were resuspended and homogenized by mixing with sterile MilliQ water and 100µL of 0.1-mm glass beads (Scientific Industries Inc., Bohemia, NY, USA), heating for five minutes at 95°C and then

vortexing at high speed for three minutes. Homogenized cells were then centrifuged and supernatants collected in 15mL conical tubes. Beads were washed a total of six times in ice cold sterile MilliQ water by vortexing and centrifuging in order extract protein, supernatants were collected and pooled after each wash. Extracted protein was mixed thoroughly and stored at -80°C. Total protein was quantified by Bicinchoninic Acid (BSA) Protein Assay Kit with a bovine serum albumin (BSA) standard (Pierce Protein Research Products, Thermo Fisher Scientific) and 100µg of protein was digested following a previously described protocol. Briefly, protein samples were digested using a filter-aided sample preparation method, using YM10 cartridges (Phenomenex, Torrence, CA, USA). Samples were digested overnight with 1.5µg of trypsin at 37°C. The following day, peptides were dried down, diluted to 100ng/µL with MS-grade H_2O, and then diluted 1/10 with nano-LC buffer A (2% acetonitrile, 0.1% formic acid). Each peptide sample was analysed using an Easy nLC II connected in-line to an LTQ Orbitrap Velos mass spectrometer, with a nanospray ion source at 2.1 kV (Thermo Fisher Scientific). The peptide sample (1µg) was loaded onto a C_{18}-reversed phase trap column (30 × 0.1 mm with 5µm particles) with 100% LC buffer A (2% acetonitrile, 0.1% formic acid), and then separated on a C_{18}-reversed phase column (1500 × 0.075 mm with 2.4µm particles) using a linear gradient of 2-32% LC buffer B (98% acetonitrile, 0.1% formic acid) over 220 min at a constant flow rate of 250 nL/min. Both columns were packed in-house with ReproSil-Pur C_{18}-AQ resin (Dr. Maisch). The full-MS survey scans were acquired in the Orbitrap over *m/z* 300-1700 with a target resolution of 60,000 at *m/z* 400. Data-dependent acquisition method was used, dynamically choosing the top 10 abundant precursor ions from each survey scan with an isolation width of *m/z* 2 for fragmentation by CID. The intensity threshold for selecting a precursor ion for fragmentation was 1000 ions, with dynamic exclusion for 15s. All spectra were processed using

Progenesis QI (2.1, Nonlinear Dynamics) and database searching was done with Mascot (v2.5, Matrix Science). Searches were performed against a NCBI subset database of *A. baumannii* strain ATCC17978 (GCA_000015425.1, 3803 sequences). Mascot search results were imported into Scaffold (v4.4, Proteome Software) and filtered using 0.1% FDR for peptides, 1.0% FDR for proteins, and at least 2 peptides per protein. The Scaffold protein identification results were imported into Progenesis QI, and all label-free protein quantitation data was exported from Progenesis QI to Excel (Microsoft) for final data analysis using ratios of AB141 against ATCC17978. Gene Ontology (GO) annotation was performed on the ATCC17978 genome using the Blast2Go tool in the Geneious software suite (http://www.geneious.com/). GO codes were translated utilizing the Gene Ontology Consortium database in Microsoft Excel software.

3.16 Construction of constitutively expressed fluorescent single-copy insertion plasmids

Constitutively expressing plasmids were constructed by truncating the *lac* repressor gene in pUC18T-miniTn*7*-Gm-LAC by digesting with *Pvu*II and *Mlu*I following the digestion procedure detailed above. Following digestion, the ends were polished using T4 DNA polymerase (New England Biolabs) following the manufacturer's instructions so the plasmid could be re-circularized. Ligation of the linearized plasmid was performed using T4 DNA Ligase (Thermo Fisher Scientific) using the manufacturer's suggested reaction conditions for self-circularization of linear DNA with 50ng of DNA. Following overnight incubation at 16°C the ligation mixture was transformed into *E. coli* DH5α and plated on LB agar supplemented with 15μg/mL gentamicin. The resultant plasmid, pPLS228, was confirmed by PCR using LacIq_Fwd and LacIq_Rev primers and restriction digestion with PvuII and BglI. The four fluorescent genes, GFP, YFP, CFP, and DsRed-Express were cloned into pPLS228 by amplifying from plasmids

DQ493881, DQ493883, DQ493882, and DQ493884 respectively (Choi and Schweizer 2006). All fragments were amplified using the same forward primer, FP_Fwd_XhoI. YFP, CFP, and DsRed-express were amplified using the same reverse primer YCR_Rev_SacI while GFP was amplified with a unique reverse primer GFP_Rev_SacI. Amplified fragments were gel purified as detailed above and the purified fragments alongside pPLS228 were digested with *Xho*I and *Sac*I. Ligation of the four fragments into pPLS228 was performed as discussed above and the ligated constructs were transformed into *E. coli* SM10 and plated on LB agar supplemented with 15μg/mL gentamicin. Fluorescing colonies were screened by PCR, and confirmed by restriction digestion with *Bgl*I and *Pst*I and Sanger sequencing. The confirmed plasmids were named pPLS236 for GFP, pPLS237 for CFP, pPLS238 for YFP, and pPLS239 for DsRed-Express. Plasmid maps are provided in Appendix 9.2.

4 Results

4.1 Creation of *adeN* deletion in ATCC17978

In order to elucidate the role of *adeN* in *A. baumannii* an unmarked deletion mutant had to be created. *adeN* was deleted in ATCC17978 using the homologous recombination method outlined above. *adeN* deletion was initially confirmed by PCR with AdeN_FL_Fwd and AdeN_FL_Rev primers which produce a 750bp product in ATCC17978 as compared to a 200bp product in AB141 (Fig.1). *adeN* deletion in AB141 was further confirmed by Sanger sequencing with AdeN_Seq_Fwd and AdeN_Seq_Rev. Sequence is provided in Appendix 9.1.1.

4.1.1 AdeN knock-out results in overexpression of the AdeIJK efflux pump

AdeN has been previously shown to regulate the AdeIJK efflux pump in *A. baumannii* (Rosenfeld et al. 2012).This was confirmed in AB141 by qRT-PCR of all three genes in the efflux pump operon with AdeI_RT_Fwd, AdeI_RT_Rev, AdeJ_RT_Fwd, AdeJ_RT_Rev and, AdeK_RT_Fwd, AdeK_RT_Rev primers (Fig. 2). AB141 shows ~3.5-fold overexpression of the entire AdeIJK efflux pump operon. Equal overexpression of all genes in the operon in response to *adeN* deletion allows us to reliably evaluate expression of the pump using a single member of the operon.

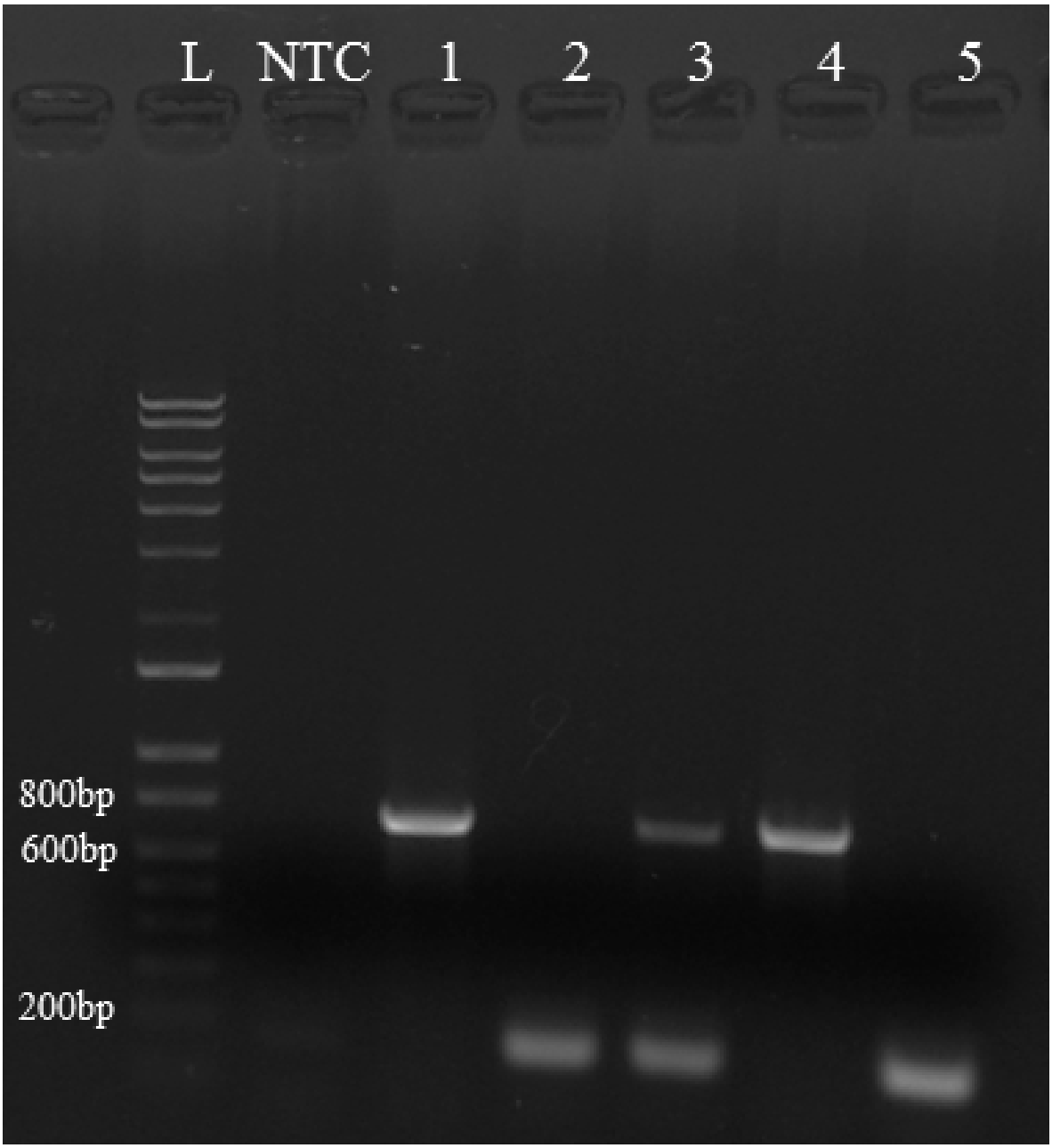

Figure 1: Gel picture of *adeN* PCR with AdeN_FL_Fwd and AdeN_FL_Rev primers. NTC = No Template Control, L = Ladder, 1 = ATCC17978, 2 = AB141, 3 = AB183, 4 = AB185, 5 = AB186. Expected product size for intact *adeN* is 750bp, expected product size for deleted *adeN* = 200bp.

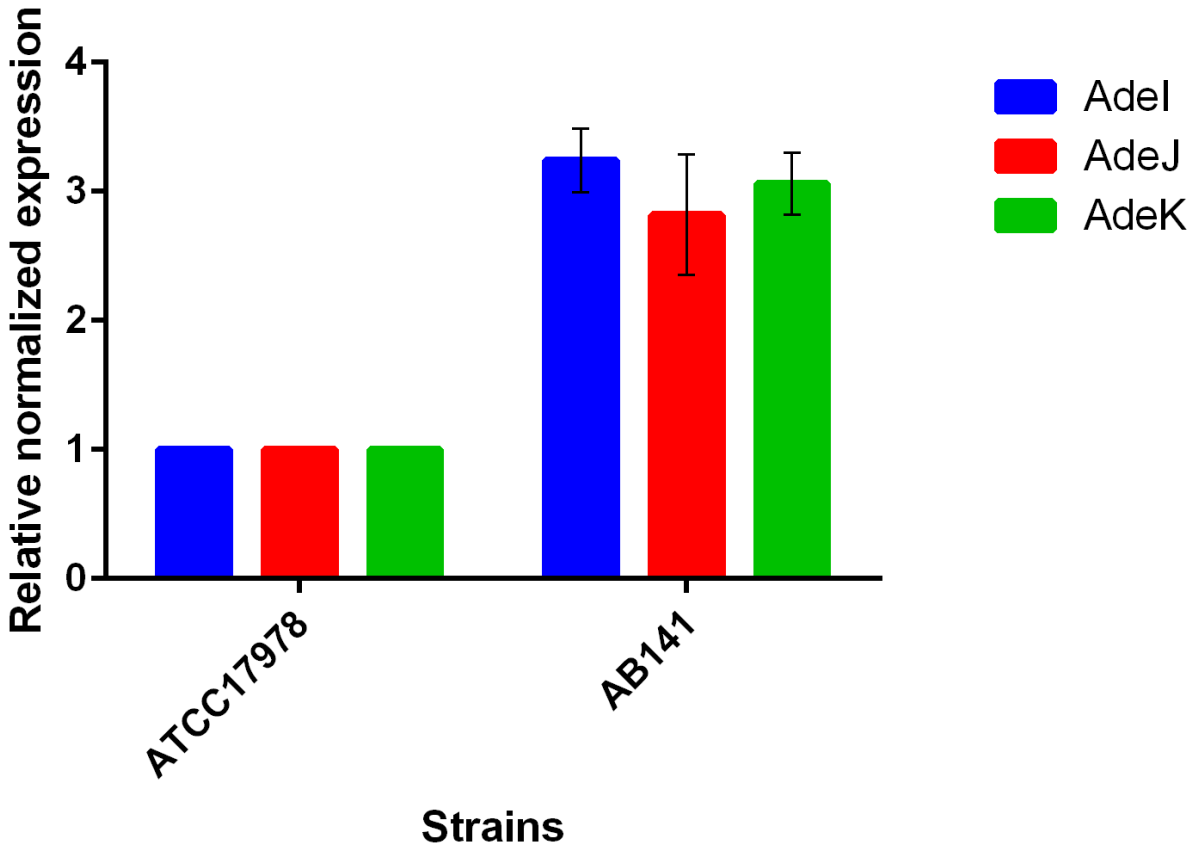

Figure 2. Relative expression of *adeI*, *adeJ* and, *adeK* in AB141 compared to the parent strain ATCC17978. AB141 shows ~3.5-fold overexpression of the AdeIJK efflux pump compared to the parental strain.

4.1.2 Complementation of *adeN* in AB141

Part of the process of confirming what phenotypes could be attributed to *adeN* was complementation. In order to try to emulate the natural condition as best as possible we decided to use a mini-Tn*7* single copy insertion system under IPTG control (Choi and Schweizer 2006). This allows *adeN* to be expressed from the chromosome under tight control. Evaluation of the complemented strain AB183 is detailed below. Complementation of *adeN* into AB141 with pPLS223 downstream of *glmS2* was confirmed by end-point PCR. To firstly identify the presence of *adeN* in the resultant AB183 strain AdeN_FL_Fwd and AdeN_FL_Rev were used (Fig.1). Secondly its insertion location downstream of *glmS2* was confirmed by use of GlmS_Fwd and Tn7_Rev primers (Fig. 3).

4.1.3 Evaluation of *adeN* and *adeIJK* expression by qRT-PCR in AB141 and AB183

Complementation of *adeN* in AB183 was further confirmed by qRT-PCR using AdeN_RT_Fwd and AdeN_RT_Rev primers to confirm *adeN* expression under 1mM IPTG induction. To confirm that *adeN* was being not only transcribed but translated as well, expression of the *adeIJK* efflux pump was evaluated by qRT-PCR. If *adeN* was being translated the *adeIJK* efflux pump should show repression. This was achieved using the AdeJ_RT_Fwd and AdeJ_RT_Rev primers as it has already been shown that the entire pump operon is expressed together (Fig. 2). Induction of *adeN* with 1mM IPTG resulted in ~17-fold overexpression of *adeN* and a resulting repression of *adeIJK* to 0.4-fold of wild-type levels (Fig. 4). AB141 was included as a control and shows 3.5-fold overexpression of *adeJ*.

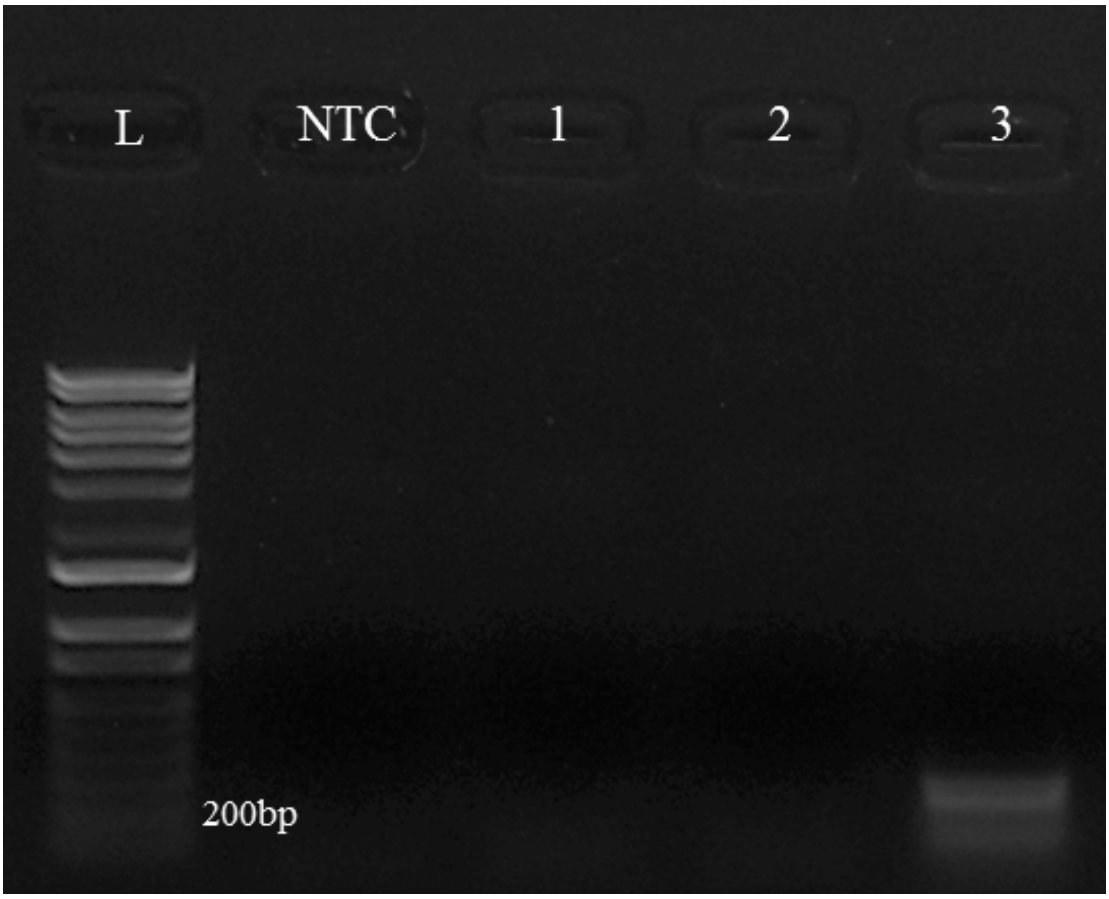

Figure 3. Gel picture of miniTn*7*-*adeN* insertion PCR with GlmS_Fwd and Tn7_Rev primers. NTC = No Template Control, L = Ladder, 1 = ATCC17978, 2 = AB141, 3 = AB183. Expected product size for miniTn*7* insertion downstream of *glmS2* = 200bp.

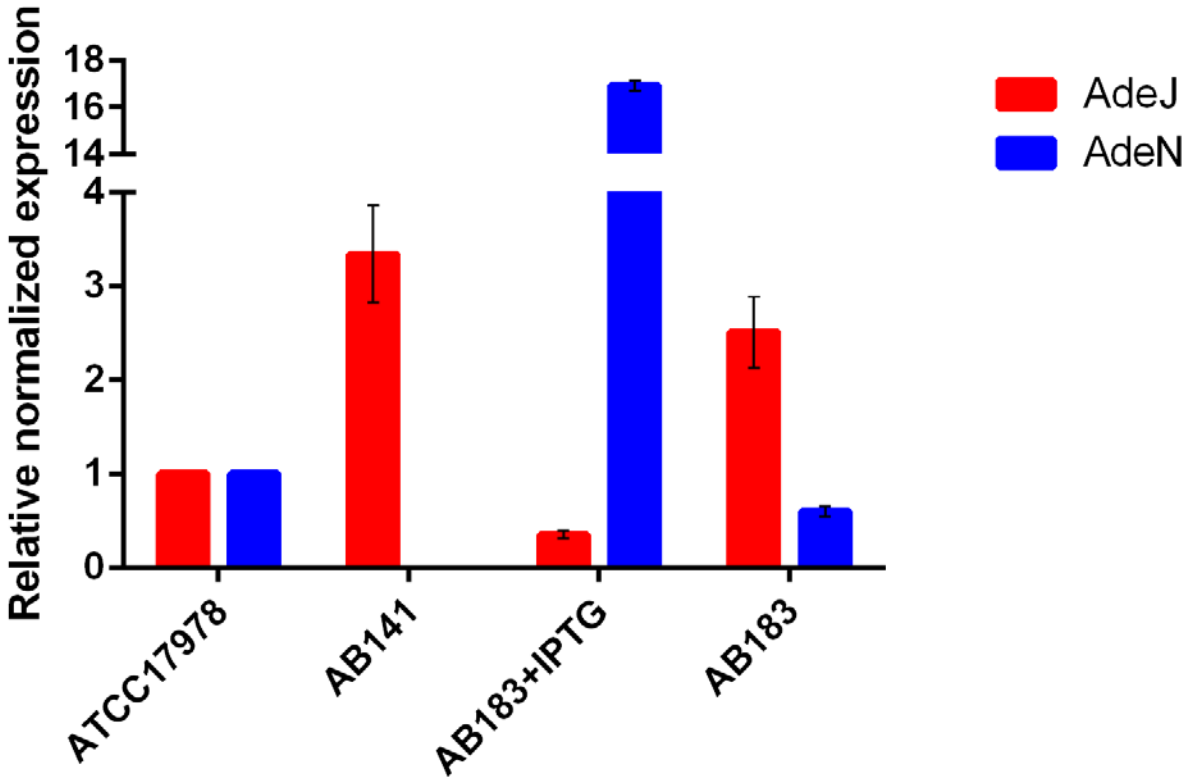

Figure 4. Relative expression of *adeN* and *adeJ* in AB141 and the compliment strain AB183 compared to the parent strain ATCC17978. AB141 shows ~3.5-fold overexpression of the AdeIJK efflux pump compared to the parental strain. Induction of AB183 with 1mM IPTG results in ~17-fold overexpression of AdeN and repression of AdeIJK to 0.4-fold of wild type ATCC17978.

4.1.4 Transcriptomic and Proteomic Analysis

To assess if AdeN may be playing a global regulatory role in *A. baumannii* we utilized a combination of RNA-Seq (Fig. 5) and proteomic (Fig. 6) analyses. In the RNA-Seq analysis we identified 106 genes that exhibited a statistically significant difference in expression of at least $1.5_{\log (2)}$-fold change in comparison to the wild-type ATCC 17978. GO analysis was able to annotate 59 out of 106 genes identified in RNA. Using proteomic analysis, we were able to detect 31 proteins that exhibited a statistically significant change of at least 2-fold. Of the 31 proteins identified 22 were annotated in our analysis.

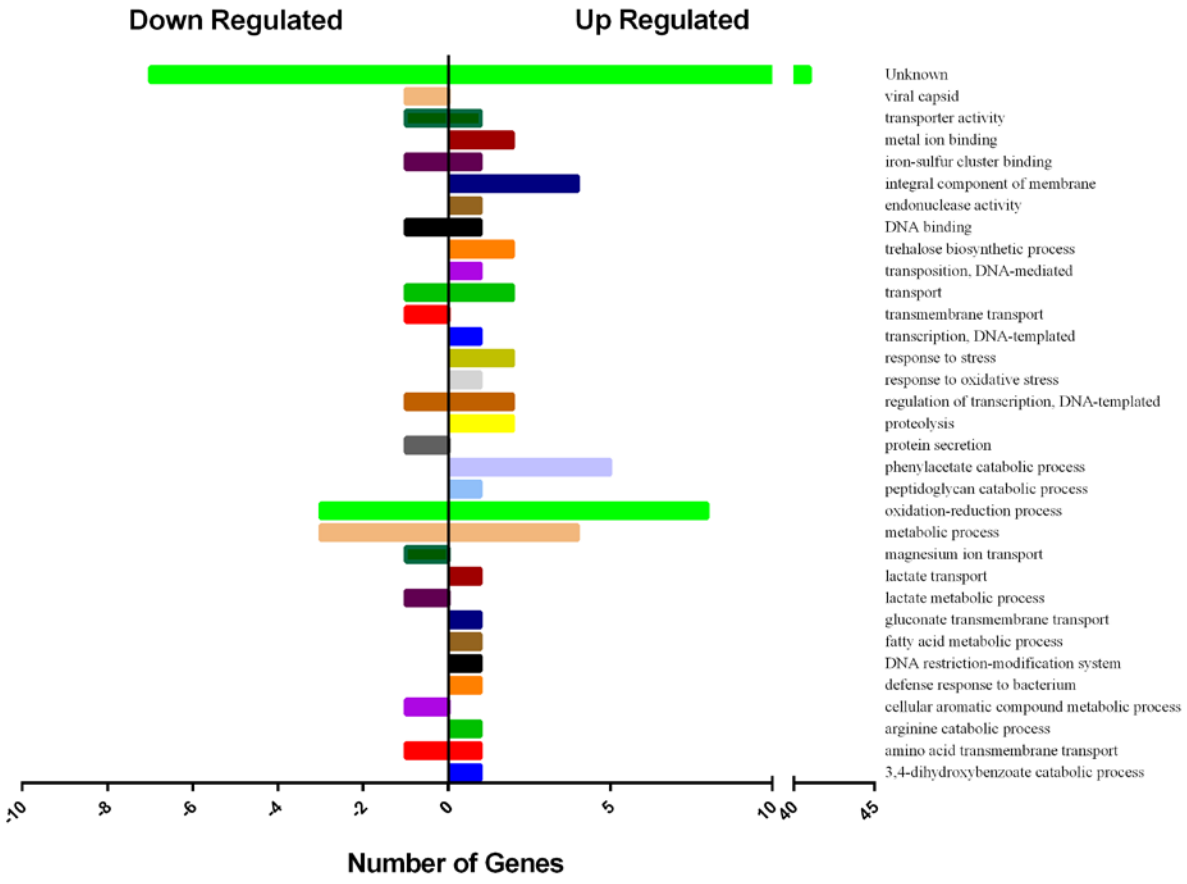

Figure 5. Gene Ontology annotation of genes whose expression was significantly altered in AB141 when compared to ATCC17978 as determined by RNA-Seq experiments. Figure shows number of genes up regulated and down regulated in each GO class. GO classes were selected based on biological process annotation. If a single gene was annotated as having more than one distinct role all annotations were reported. Unannotated genes were listed as Unknown.

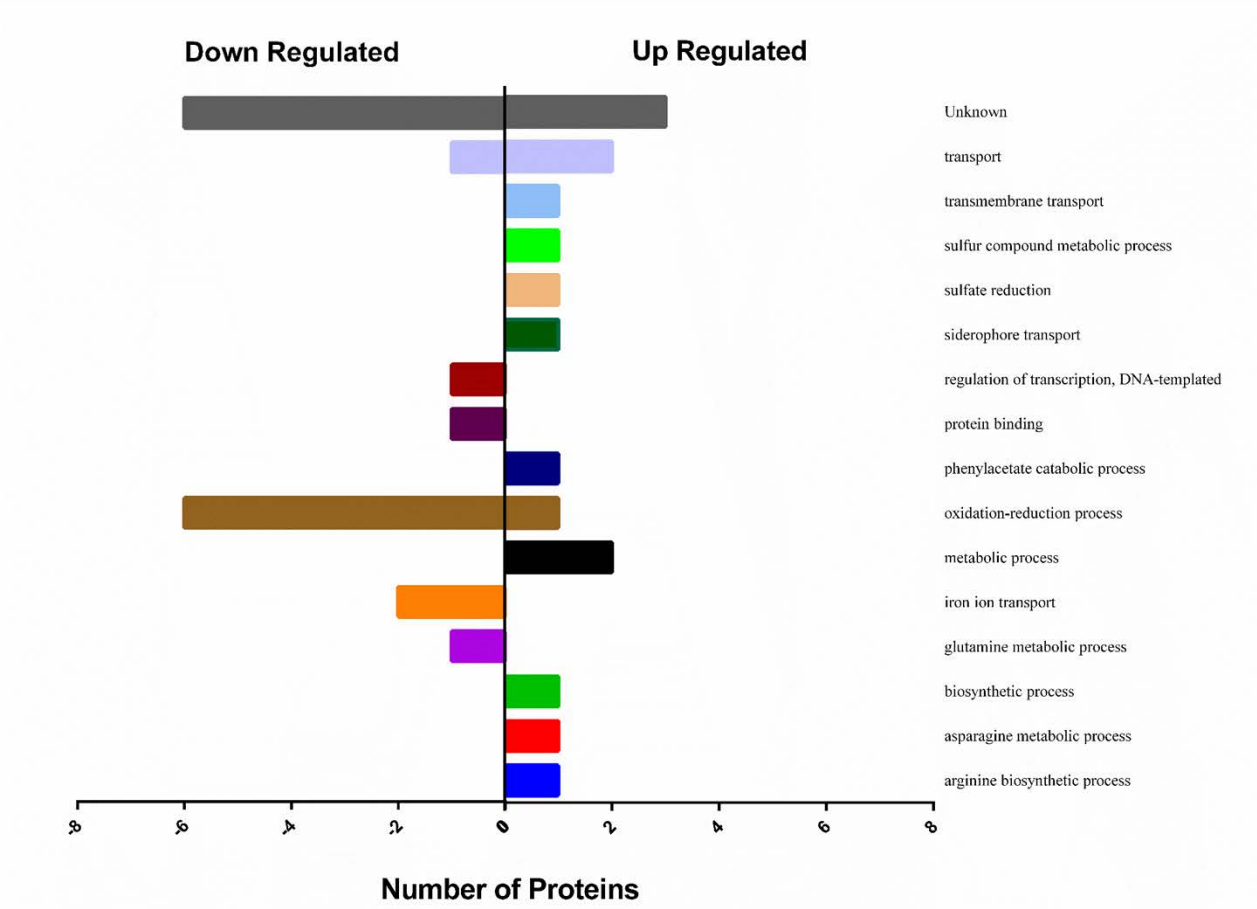

Figure 6. Gene Ontology annotation of proteins whose expression was significantly altered in AB141 when compared to ATCC17978 as determined by proteomic experiments. Figure shows number of proteins up regulated and down regulated in each GO class. GO classes were selected based on biological process annotation. If a single protein was annotated as having more than one distinct role all annotations were reported. Unannotated proteins were listed as Unknown.

4.2 *adeIJK* deletion in ATCC17978 and AB141

In order to determine whether the phenotypes being observed in the *adeN* deletion mutant AB141 were due to loss of *adeN* expression and not the resultant overexpression of *adeIJK*, an *adeIJK* deletion mutant was created in both the wild-type and *adeN* deletion backgrounds. The confirmation details of the two *adeIJK* deletion mutants, AB185 and AB186 respectively, are discussed below.

adeIJK deletion in ATCC17978 (AB185) and AB141 (AB186) was initially confirmed using end-point PCR with AdeIJK_FL_Fwd and AdeIJK_FL_Rev primers (Fig. 7). Putative deletion mutants produced a 743bp product whereas wild-type strains would not give a product due to the size of the pump operon (6.2kb). Because of the inability to reliably amplify the 6.2kb wild-type product in conjunction with the 743bp knockout product this full length PCR was used in combination with an internal *adeJ* end-point PCR using AdeJ_Int_Fwd and AdeJ_Int_Rev primers. This PCR reaction would produce a 1kb product in wild-type strains and no product in the mutant strains. The combination of these two PCR reactions, a full length reaction and an internal reaction, provided a reliable screen for putative operon deletions.

adeIJK deletions in AB185 and AB186 were further confirmed by Sanger sequencing. Sequence is given in Appendix 9.1.2 and 9.1.3 respectively.

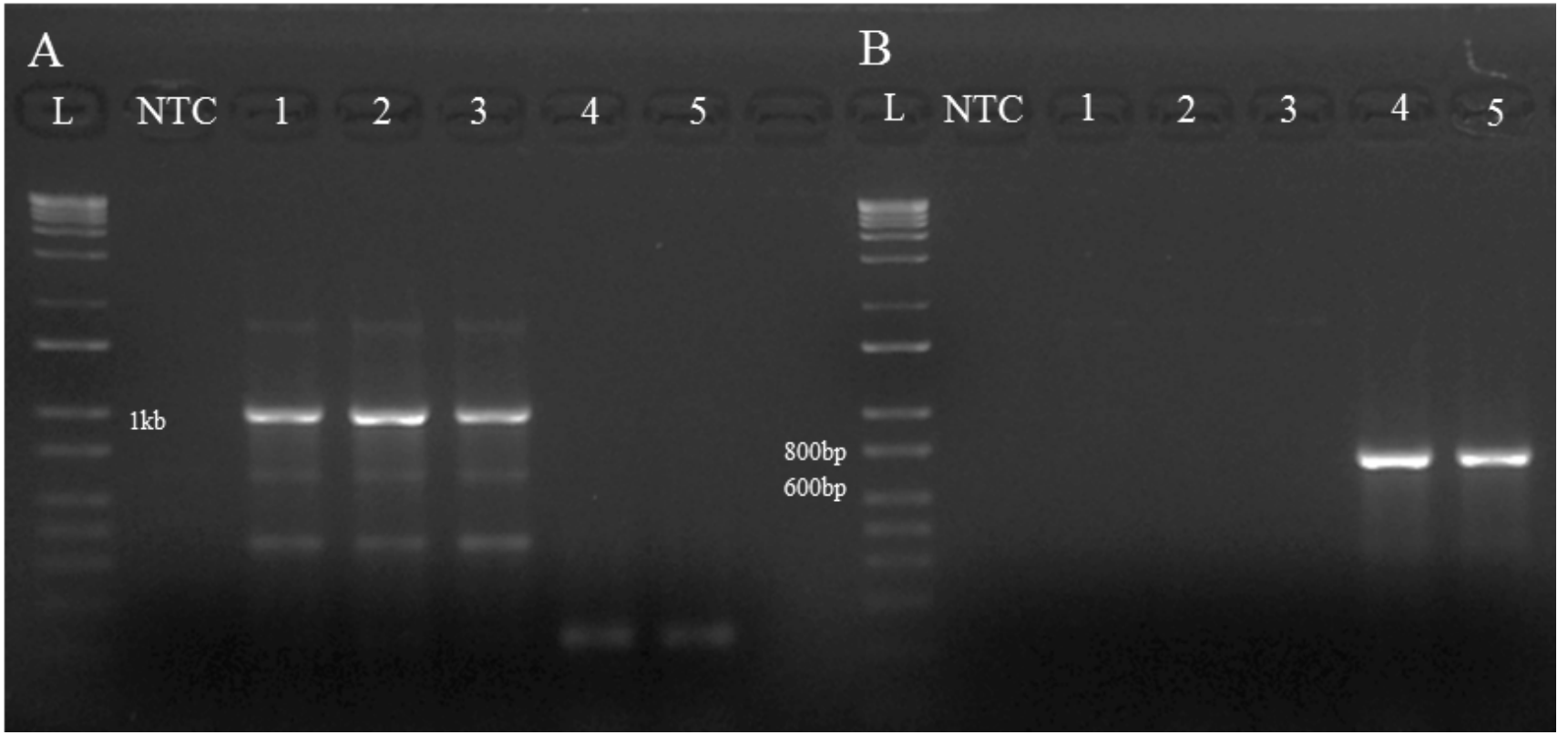

Figure 7: (A) Gel picture of *adeJ* PCR with AdeJ_Int_Fwd and AdeJ_Int_Rev primers. NTC = No Template Control, L = Ladder, 1 = ATCC17978, 2 = AB141, 3 = AB183, 4 = AB185, 5 = AB186. Expected product size if *adeJ* intact = 1003bp. (B) Gel picture of *adeIJK* PCR with AdeIJK_FL_Fwd and AdeIJK_FL_Rev primers. NTC = No Template Control, L = Ladder, 1 = ATCC17978, 2 = AB141, 3 = AB183, 4 = AB185, 5 = AB186. Expected product size if *adeIJK* deleted = 743bp

4.3 Phenotypic Characterization of *adeN* and *adeIJK* deletion mutants

4.3.1 Minimum Inhibitory Concentrations

To assess whether or not the gene deletions we had performed were having a phenotypic effect minimum inhibitory concentrations were performed for fluoroquinolones, known substrates of the AdeIJK efflux pump that have been previously shown to respond to *adeN* deletion (Rosenfeld et al. 2012). As expected the *adeN* deletion mutant AB141 exhibits a 4-fold decrease in susceptibility to both moxifloxacin and ciprofloxacin compared to the wild-type ATCC17978 (Table 3). IPTG induction of the complement strain AB183 restores susceptibility to within 2-fold of wild-type levels. Predictably *adeIJK* deletion mutants AB185 and AB186 exhibit increased susceptibility to fluoroquinolones, 2-fold in the case of moxifloxacin and 6-fold in the case of ciprofloxacin.

4.3.2 Twitching Motility

Having established that the *adeN* and *adeIJK* deletion mutants were exhibiting the expected phenotypes previously attributed to the mutations we began to test other phenotypic characteristics associated with virulence that had not been previously shown to be linked to *adeN* or *adeIJK* deletion, the first of which was twitching motility. While *A. baumannii* is classified as being non-motile due to its lack of flagella it has been shown to exhibit twitching motility via a type-IV pillus (Harding et al. 2013). As such we evaluated twitching motility in all the generated mutant strains by growth in semi-solid agar (0.3%) (Fig. 8). All three gene deletion mutants show a 70-80% reduction in motility compared to the wild-type ATCC17978. Induction of the complemented strain AB183 with 1mM IPTG results in restored motility to near wild-type levels.

Table 3. Minimum Inhibitory Concentrations against fluoroquinolones in μg/mL. Mox; moxifloxacin, Cip; Ciprofloxacin

Strain	Mox	Cip
ATCC17978	0.0625	0.25
AB141	0.25	1
AB183+IPTG	0.03125	0.125
AB183	0.125	0.5
AB186	0.03125	0.03125

A

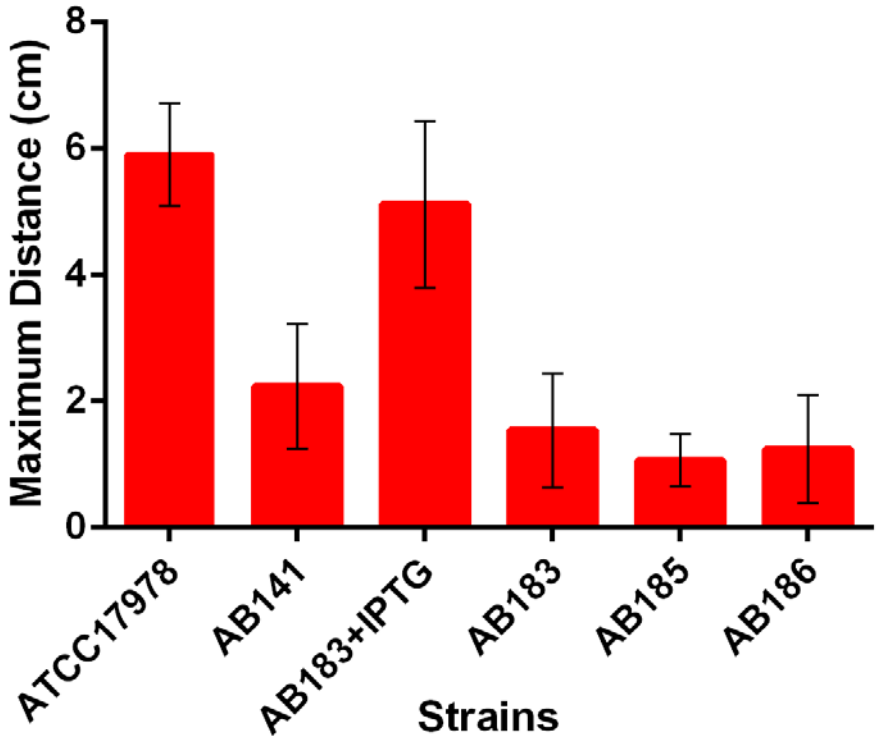

B

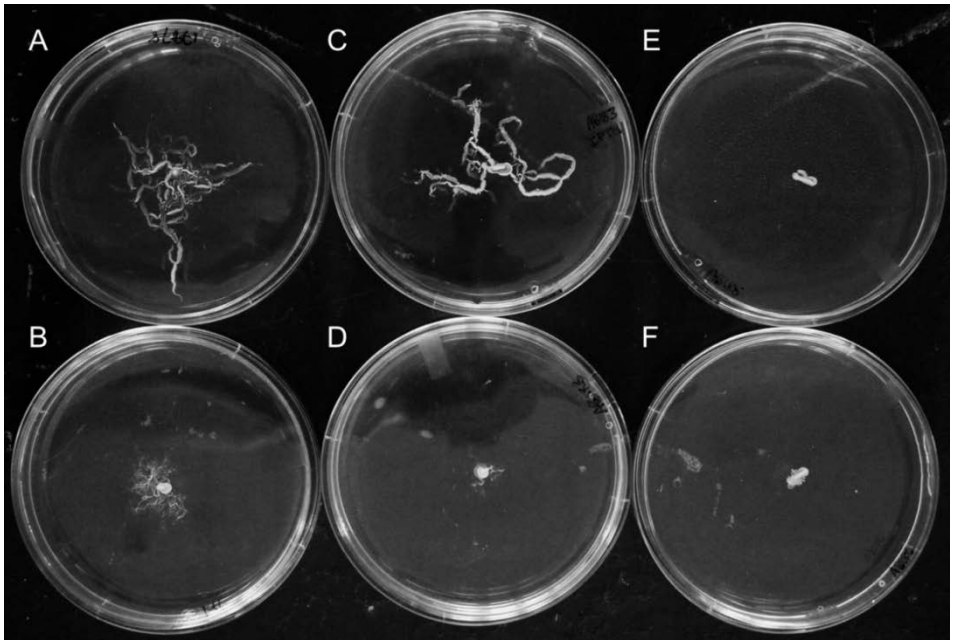

Figure 8. (A) Motility of ATCC17978(WT), AB141(Δ*adeN*), AB183+IPTG(AB141-*adeN*), AB183 AB141-*adeN*), AB185(Δ*adeIJK*) and, AB186(AB141Δ*adeIJK*) in semi-solid agar. All strains, apart from the induced compliment, show decreased motility relative to ATCC17978. (B) Representative plates for each strain tested. A: ATCC17978, B: AB141, C: AB183+IPTG, D: AB183, E: AB185, F: AB186

4.3.3 Biofilm Formation

The ability to create biofilms is one of the most significant factors that allows *A. baumannii* to persist in the hospital environment (Peleg et al. 2008) and this phenotype has been previously linked to *adeN* (Saranathan et al. 2017). As this is such an important phenotype contributing to the clinical significance of *A. baumannii* biofilm formation was evaluated in the *adeN* and *adeIJK* deletion mutants (Fig. 9).

All three *adeN* and *adeIJK* deletion mutants showed 70-80% reduction in biofilm formation in comparison to the ATCC17978.

4.3.4 Virulence in *Galleria mellonella*

After observing attenuation of cell motility and biofilm formation in the deletion mutants we wanted to see if attenuation of these phenotypes translated to decrease killing in a *Galleria mellonella* model.

Deletion of *adeN* results in attenuation of virulence compared to the wild-type ATCC17978 with AB141 showing 80% survival compared to 10% survival in ATCC17978 (Fig. 10A). We were able to partially restore virulence by IPTG induction of the complement strain AB183 which showed 50% survival ($p<0.05$). However, comparison of the *adeN* and *adeIJK* deletion mutants AB141, AB185, and AB186 show no significant difference in virulence (Fig. 10B).

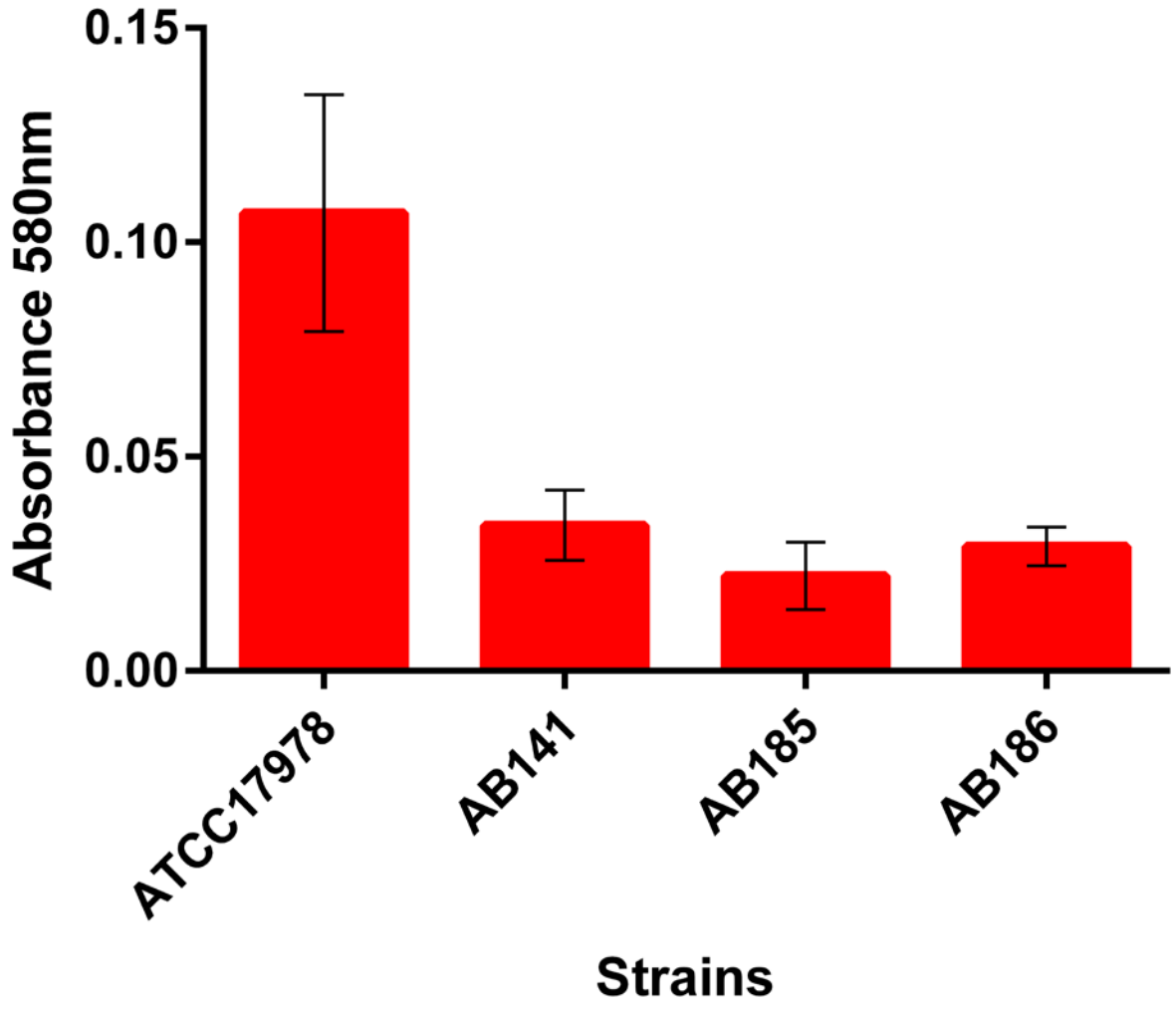

Figure 9. Biofilm formation by *adeN* and *adeIJK* deletion mutants. Biofilm formation was monitored after 48 hours and biofilms were quantified by measuring the optical density at 580 nm. ATCC17978 was used as the control. Significant decrease ($p<0.01$) was confirmed by student t-test.

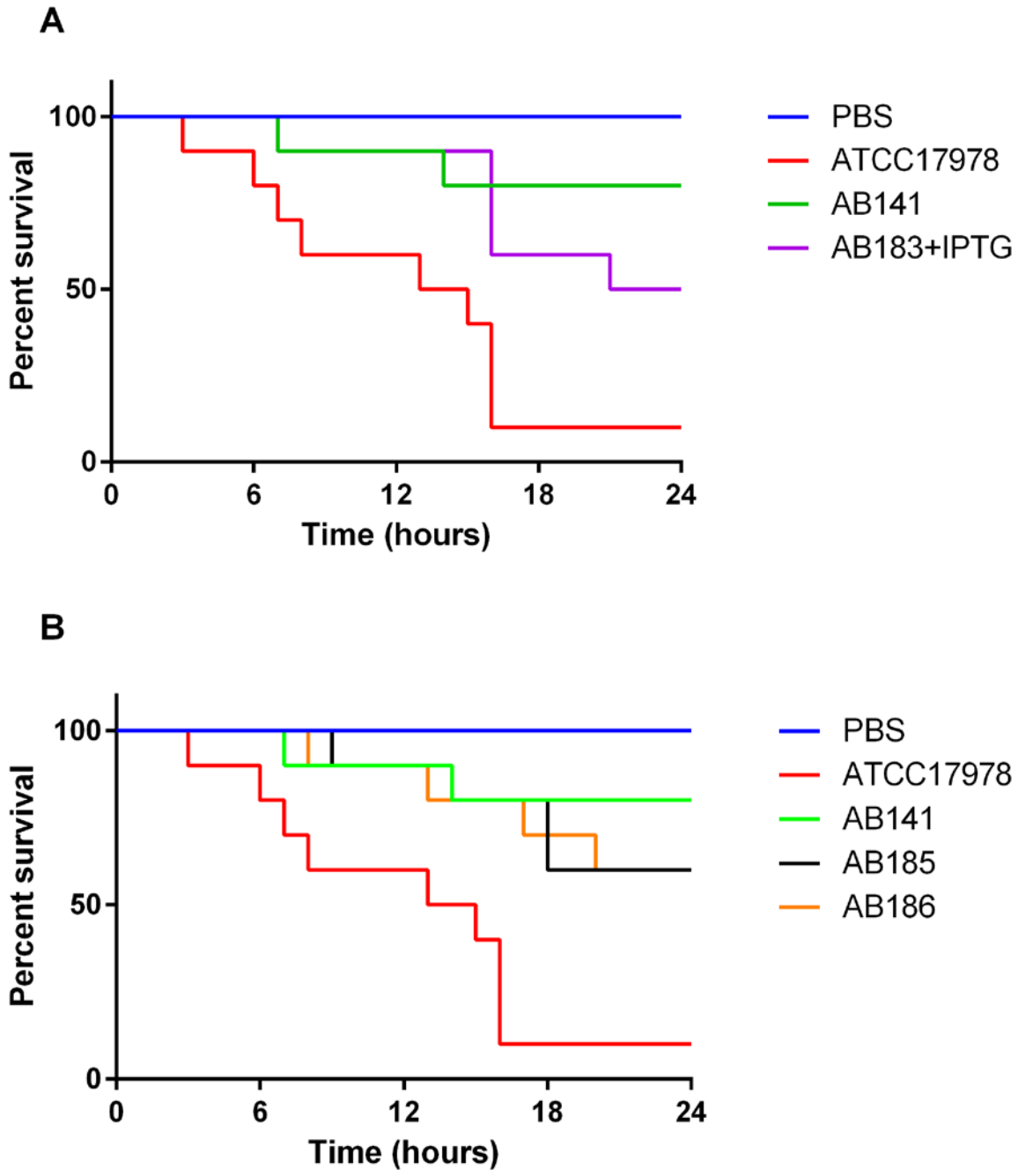

Figure 10. Virulence in *Galleria mellonella* infection assays. (A) *adeN* deletion (AB141) results in attenuated virulence (80% survival) compared to wild-type (10% survival). Complementation (AB183) results in partial return of virulence with 50% of worms surviving ($p<0.05$). (B) All mutants show attenuated virulence compared to wild-type however differences between *adeN* deletion (AB141), *adeIJK* deletion (AB185) and the double mutant (AB186) were not statistically significant as both *adeIJK* mutants showed (60% survival) ($p>0.05$).

4.3.5 Fatty Acid Composition

Previous study of the triclosan resistant mutant AB042 by Fernando *et al.* showed a restructuring of the cellular membrane which could be potentially linked to AdeN and or AdeIJK (Fernando et al. 2017). To determine if this was the case cellular membrane fatty acid composition was evaluated in all mutant strains and the wild-type ATCC17978 by gas chromatography (Fig. 11).

All three deletion mutants AB141, AB185, and AB186 show a shift in membrane composition compared to ATCC17978. The three mutants show a distinct shift from main membrane constituents C15:1 and C18:1n11t to C16:0 and C18:1n9 which indicates a shift from a more fluid membrane to a more rigid membrane.

4.3.6 Growth Curves

After observing the shift in membrane composition shown by AB141, AB185, and AB186, we were curious if the more rigid membrane composition exhibited by the mutant strains would result in an increased tolerance to osmotic stress. Firstly, growth of the mutant strains was evaluated to see if the deletion of *adeN* or *adeIJK* resulted in any significant growth defects under non-stress condition (Fig. 12A). In LB broth none of the deletion mutants showed any significant growth defects compared to the wild-type ATCC17978. However, when the growth media was supplemented with 5M sucrose to induce osmotic stress AB141 and AB185 show increased tolerance compared to the wild-type ATCC17978 after 8 hours ($p<0.01$) while AB186 showed the same susceptible phenotype as ATCC17978 (Fig. 12B).

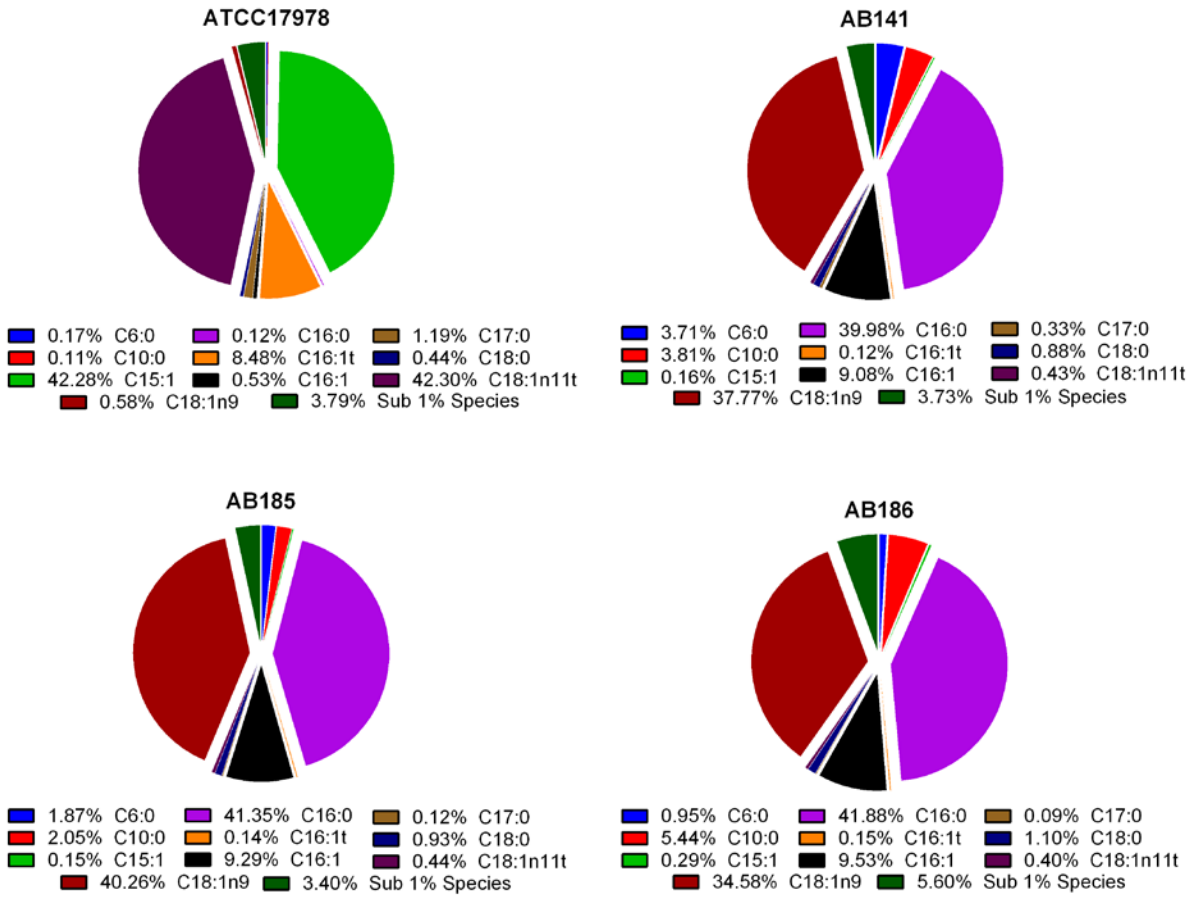

Figure 11. Fatty acid composition of *adeN*, and *adeIJK* deletion mutants in comparison to the wild-type ATCC17978. The three mutants show a distinct shift from main membrane constituents C15:1 and C18:1n11t to C16:0 and C18:1n9.

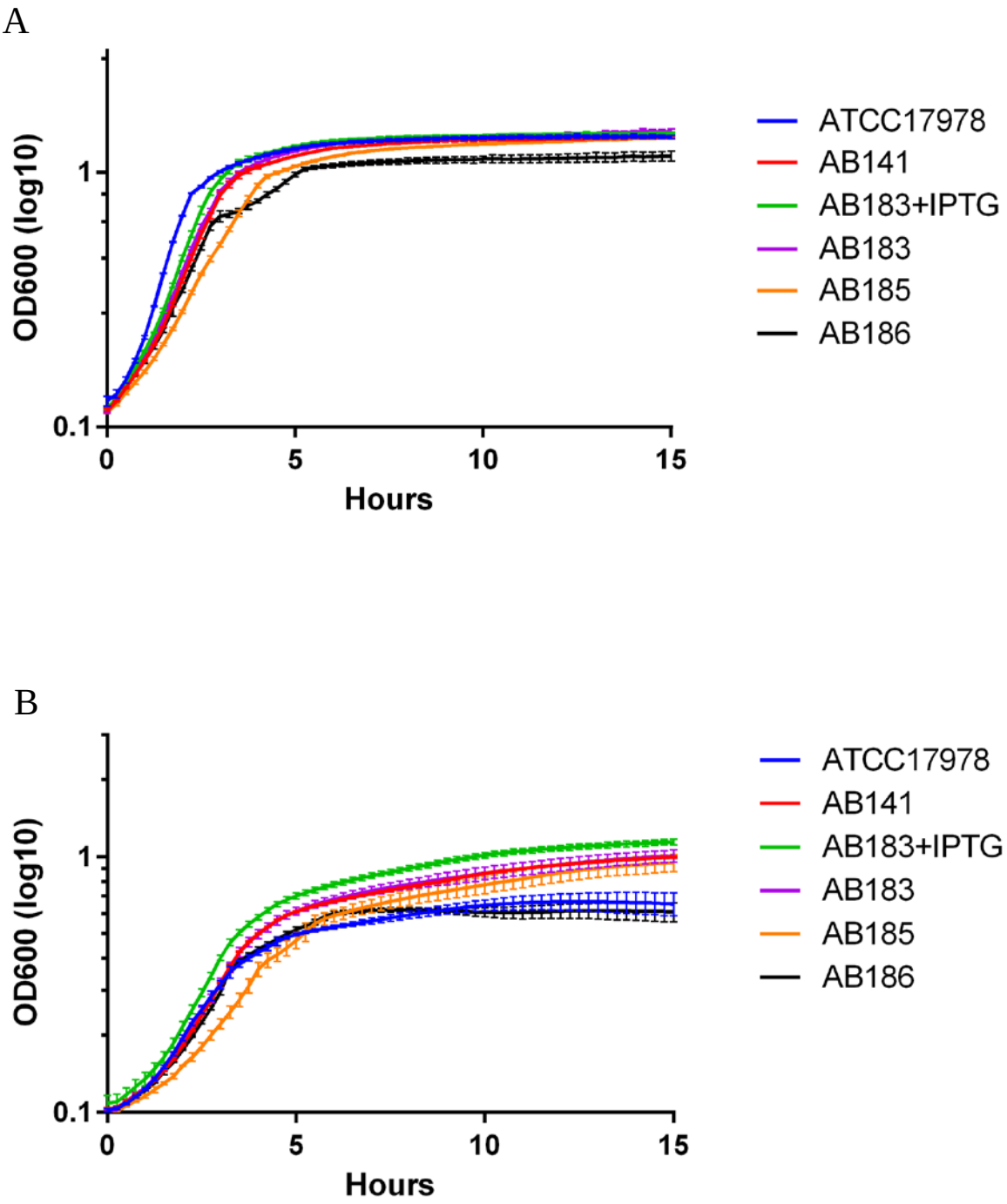

Figure 12. (A) Shows the growth of all strains in LB medium. (B) Evaluation of osmotic stress tolerance of *adeN* and *adeIJK* deletion mutants. AB141 and AB185 show a statistically significant improved fitness when compared to the parent strain ATCC17978 under osmotic stress conditions (0.5M sucrose) after 8 hours ($p<0.01$). Growth was monitored for 24 hours at 37 ºC with continuous shaking. Data shown is representative of two biological replicates.

4.3.7 Scanning Electron Microscopy

The AdeIJK efflux pump is the only currently characterized RND-efflux pump in *A. baumannii* that is conserved through all members of the species and is constitutively expressed in all strains (Damier-Piolle et al. 2008b) and as efflux pumps are a major membrane constituent we hypothesized that AdeIJK may play an important role in the cellular structure of *A. baumannii.* In order to assess this scanning electron microscopy was performed on the *adeN* and *adeIJK* deletion mutants as well as the wild-type ATCC17978 (Fig. 13). Scanning electron microscopy showed that while the *adeN* deletion mutant AB141 which exhibits ~3.5-fold overexpression of AdeIJK showed no difference in cell structure compared to ATCC17978, However the *adeIJK* deletion mutants AB185 and AB186 exhibited a rounding of the cells in comparison to the rod shaped ATCC17978 and AB141.

4.3.8 Evaluation of *adeN* and *adeJ* expression in AB185 by qRT-PCR

To explain why AB141 and AB185 were showing similar phenotypes despite opposing expression levels of the AdeIJK efflux pump expression of *adeN* and *adeJ* were determined in AB185 by qRT-PCR (Fig. 14). As expected, expression of *adeJ* was completely abolished in AB185 due to *adeIJK* deletion. However interestingly AB185 exhibited 0.3-fold repression of *adeN*.

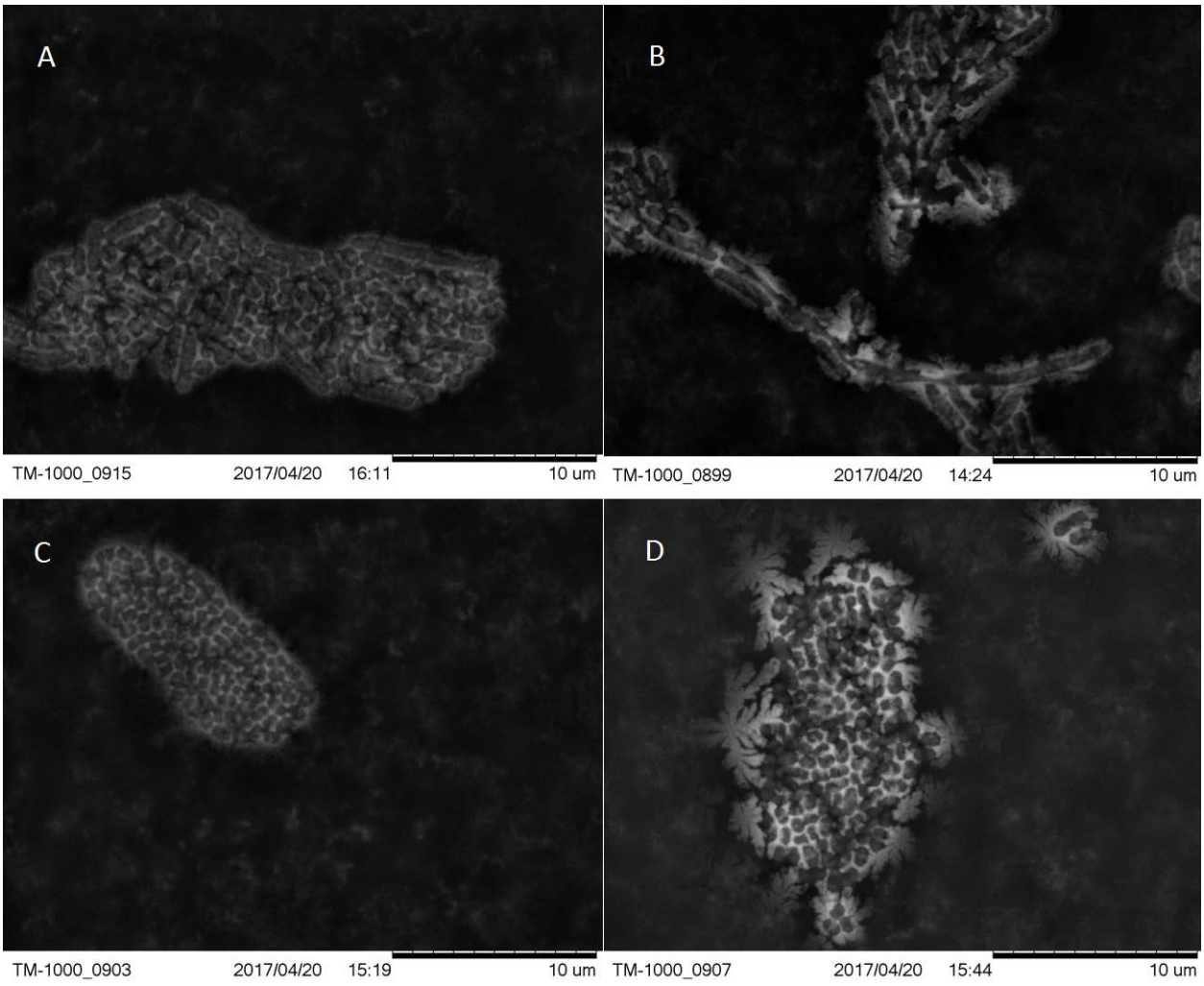

Figure 13. Scanning electron microscopy of *adeN* and *adeIJK* deletion mutants (A) ATCC17978, (B) AB141, (C) AB185, (D) AB186. *adeIJK* deletion mutants AB185 and AB186 show a more rounded cell morphotype compared to ATCC17978 and AB141.

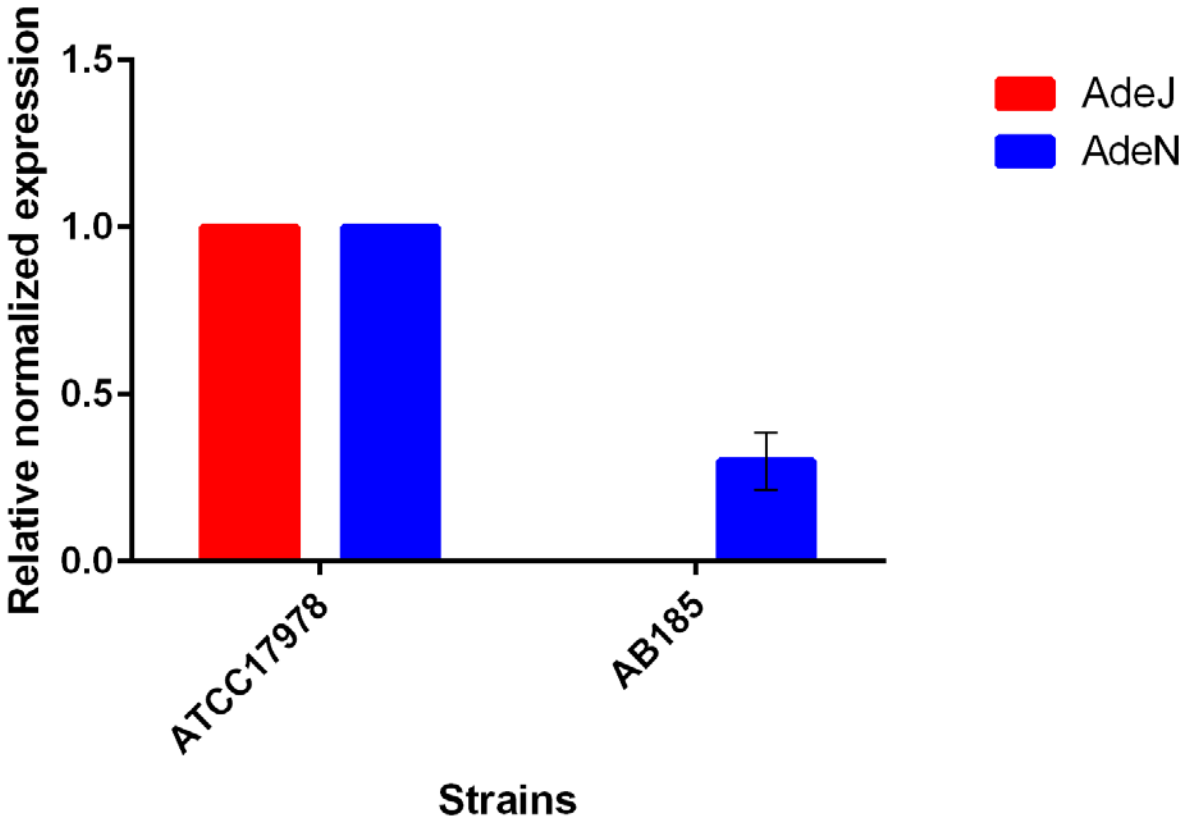

Figure 14. Relative expression of *adeN* and *adeJ* in AB185 by qRT-PCR. AB185 shows abolished expression of *adeJ* as expected. AB185 also shows 0.3-fold repression of *adeN* compared to ATCC17978.

4.4 Fluorescent single copy insertion plasmids

The constructed plasmids pPLS236, pPLS237, pPLS238, and pPLS239 were transformed into *E. coli* SM10 cells and checked for fluorescence utilizing a BLooK LED Transilluminator (GeneDirex, Taoyuan City, Taiwan, China) (Fig. 15). All four constructs show high level fluorescence when exposed to transillumination.

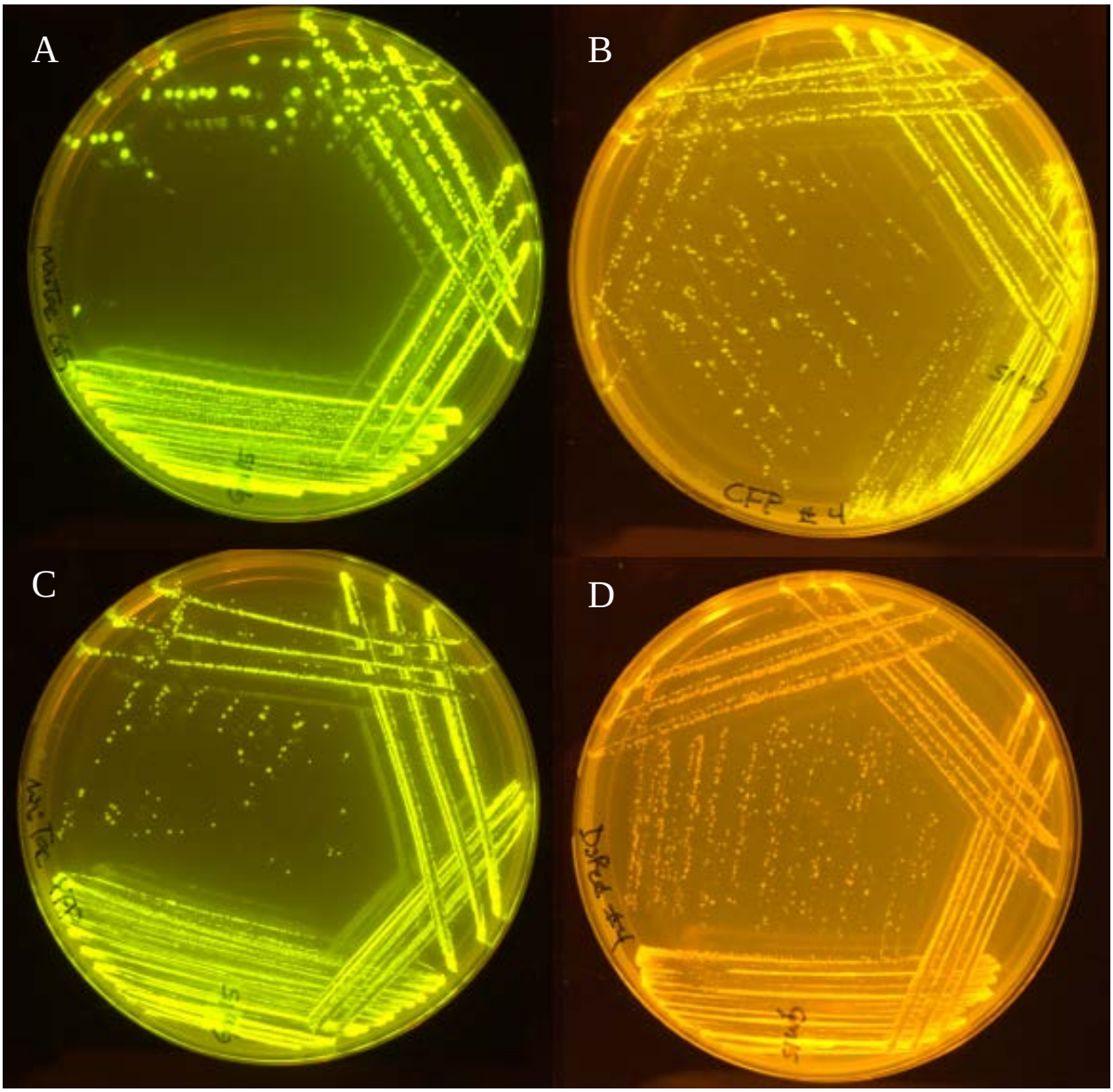

Figure 15. LED transillumination of *E. coli* SM10 containing (A) pPLS236, (B) pPLS237, (C) pPLS238, (D) and pPLS239 respectively. All constructs exhibit constitutive high level fluorescence.

5 Discussion

With increasing reports of multidrug resistance in *A. baumannii*, there is an interest in characterizing the transcriptional regulators that influence antibiotic resistance and virulence in this organism. Characterization of these regulators will not only provide insights into how *A. baumannii* develops resistance to antibiotics, but these can also serve as potential new drug targets. Indeed, some recent publications have described transcriptional regulators, particularly those belonging to the two-component regulatory systems, that appear to regulate antibiotic resistance and virulence of *A. baumannii* (Richmond *et al.*, 2016; Russo *et al.*, 2016).
In this study we show that AdeN, a TetR-family regulator that has been previously shown to regulate the expression of AdeIJK efflux pump (Rosenfeld *et al.*, 2012), also plays a role in biofilm formation, twitching motility, virulence (in *G. mellonella* model), and a variety of other cellular processes in *A. baumannii*.

To study the role that *adeN* plays in *A. baumannii* we created four strains. Firstly, a deletion mutant of *adeN* in ATCC17978 (AB141) was created. This deletion mutant was complemented via a single-copy chromosomal insertion (AB183) using a mini-Tn*7* system under IPTG inducible synthetic P_{tac} promoter. The next clear question was how to determine what observed phenotypic changes could be attributed directly to AdeN and which were caused by the resultant overexpression of the AdeIJK efflux pump shown in *adeN* deletion mutants. To help answer this question we created an *adeIJK* deletion mutant (AB185) and a double mutant of *adeN* and *adeIJK* (AB186). Comparison of these two additional deletion mutants with AB141 gives us insight into the relationship between AdeN and AdeIJK pertaining to the phenotypes tested.

When AB141 and AB186 (Δ*adeN* Δ*adeIJK*) exhibit the same phenotype and AB185 (Δ*adeIJK*) differs the tested phenotype can be attributed directly to the action of AdeN and is

independent of AdeIJK. Conversely if AB185 and AB186 exhibit a similar phenotype that differs from AB141 it indicates that the tested phenotype is dependent on AdeIJK. Lastly if AB141 and AB185 exhibit similar phenotypes that differ from AB186 this indicates that both AdeN and AdeIJK are involved. Working with these strains we tested a variety of virulence and resistance associated phenotypes to try and assess AdeN's role in *A. baumannii.*

AdeNs role as a global regulator was shown through the use of a combination of transcriptomics and proteomics.

As expected the *adeN* deletion mutant AB141 displayed a roughly 3.5-fold increase in the expression of the AdeIJK efflux pump (Fig. 2) along with a concomitant decrease in susceptibility to ciprofloxacin and moxifloxacin (Table 3) both of which are known substrates of the AdeIJK efflux pump (Fernando et al. 2014). The expression of *adeJ* (Fig. 4) as well as the susceptibility to antibiotics (Table 3) was restored to below wild-type levels once *adeN* was complemented back in AB183 by IPTG induction.

In addition to the expected decrease in antibiotic susceptibility exhibited by AB141, we also observed decreases in biofilm formation, which has been shown to be associated with AdeN previously (Saranathan et al. 2017), and twitching motility. Biofilm formation (Fig. 9) and twitching motility (Fig. 8) both exhibited a roughly 70-80% reduction in all three mutant strains compared to the wild-type ATCC17978. Motility was restored to near wild-type levels by IPTG induction of the complement strain AB183.

As both biofilm formation and twitching motility are important virulence factors, we decided to test the virulence of AB141 in *G. mellonella,* a well-accepted model to study virulence of organisms like *A. baumannii* (Peleg *et al.*, 2009). Again, all three deletion mutants exhibited attenuated virulence when compared to the parental strain which showed a 10%

survival rate, AB141 exhibiting 80% survival and both *adeIJK* mutants allowing 60% survival (Fig. 10). Complementation partially restored the virulent phenotype in AB183 which showed a 50% survival rate. This was an especially interesting finding as it is contrary to previously published data wherein another *adeN* mutant in the ATCC17978 host background exhibited increased virulence (Saranathan et al. 2017).

As discussed above this study was designed with the intention to utilize the three mutant strains to try and determine which phenotypes were dependent on AdeIJK and those that weren't. However, through the study all three mutants often exhibited the same phenotype contrary to our expectations. This was particularly confusing as the *adeN* deletion mutant AB141, and the *adeIJK* deletion mutant AB185 exhibited the same phenotype despite opposing expression of the AdeIJK efflux pump, 3.5-fold overexpression in the case of AB141 and no expression in AB185. In order to try to explain this unexpected finding AdeN expression was evaluated in AB185.

Unexpectedly AB185 exhibited 0.3-fold repression of AdeN compared to the wild-type ATCC17978 (Fig. 14). This finding, while unexpected, allows us to explain the phenotypic similarities between AB185 and AB141 due to the significant reduction in AdeN expression to 0.3-fold of wild-type shown by AB185 it seems reasonable that this would result in a mimicked phenotype. This finding was also exciting as it suggests that a novel feedback loop exists between the AdeIJK efflux pump and its regulator AdeN. This possible feedback could be an indirect effect of AdeIJK deletion.

We did observe a change in the morphology of *A. baumannii* upon deletion of the AdeIJK pump (Fig. 13), and it is possible that the downregulation of *adeN* is simply a response to this change. However how this feedback loop operates requires further study as far as its potential effect on the resistance and virulence associate phenotypes discussed in this study.

Repression of AdeN in response to *adeIJK* deletion also provides a potential answer to the matching virulence associated phenotypes observed in AB141 and AB185 further suggesting that these phenotypes are AdeN-dependent however to confirm this and understand the mechanism of AdeN repression in AB185 will require further study.

In a recent study, we showed that a triclosan-resistant mutant of *A. baumannii* showed an altered membrane lipid profile (Fernando et al. 2017). In addition to mutations in *fabI* and *fabB,* this mutant also contains a deletion in *adeN*. To investigate if the deletion of *adeN* is linked to the changes in the membrane lipid profile of *A. baumannii*, we carried out membrane lipid analysis of AB141, AB185, and AB186 and the parental ATCC17978.

We observed a significant change in fatty acid composition of all three mutant strains in comparison to the parental strain (Fig. 11) once again mimicking the phenotypic trends shown previously. Cell membranes of the mutant strains exhibited a general shift from unsaturated fatty acids to saturated fatty acids. Main constituents of the ATCC17978 membrane, C18:1n11t and C15:1, were almost completely replaced by C18:1n9 and C16:0 in the *adeN* and *adeIJK* deletion mutants. A change from a cis-unsaturated C15:1 lipid to C16:0 would result in a decrease in membrane fluidity as shorter chain length and unsaturated fatty acids are both factors associated with increased membrane fluidity (Gennis 1989). The change from C18:1n11t, a trans-unsaturated fatty acid, to the cis-unsaturated C18:1n9 would result in increased membrane fluidity as the cis-double bonded fatty acids have a greater effect on membrane fluidity than trans-double bonded fatty acids thanks to the cis-double bond causing a larger kink in the fatty acid carbon chain which impacts lipid packing (Gennis 1989). However increased chain length does attenuate the effect of unsaturation on membrane fluidity due to an increase in van der waals interactions between adjacent lipids afforded by increased chain length (Gennis 1989).

Therefore, the net effect of the fatty acid composition changes exhibited by the *adeN* and *adeIJK* deletion mutants would result in a net decrease in membrane fluidity compared to the wild-type ATCC17978.

These types of changes in membrane fluidity have been previously shown as a stress response mechanism of Gram-negative bacteria to multiple types of stress (Zhang & Rock, 2008). This potentially explains AB141 and AB185's tolerance to osmotic stress (Fig. 12), as we observed that even though AB141 and AB185 grow equally well as the parent strain in LB medium, both deletion mutants show decreased susceptiblity to osmotic stress compared to the parent. However the susceptibility exhibited by the double mutant AB186 indicates that the osmotic stress tolerance phenotype may be at least partially dependent on AdeIJK as well as AdeN.

Since AB141 showed differences in biofilm formation, twitching motility, virulence, and also the membrane lipid composition in addition to antibiotic susceptibility, we decided to explore how AdeN may be controlling these phenotypes in *A. baumannii*. To do this we utilized a combination of transcriptomic and proteomic analysis. Using these two methadologys in combination allowed us to acheive a comprehensive view of the role that AdeN plays in *A. baumannii*. Together both these approaches can serve as powerful tools to study global changes in bacterial systems. RNA-Seq is a highly sensitive method which combined with proteomics approaches, can provide biologically relevant information, particularly as the correlation between abundances of proteins and their corresponding mRNAs are not always strong, with variations as high as 60% having been previously reported (Maier *et al.*, 2009).

RNA-Sequencing of AB141 identified 106 genes that exhibited a statistically significant difference in expression or at least a $1.5_{\log(2)}$-fold change compared to the wild-type ATCC 17978. A list of these genes is provided in Appendix 9.3.1. Of the 106 genes identified in the RNA-Seq analysis 59 genes were annotated by GO analysis (Fig. 5). Using proteomic analysis, we detected 31 significantly changed proteins (1.5-fold change) out of which 22 are annotated by GO (Fig. 6). A list of identified proteins is provided in Appendix 9.3.2. However, given that a significant portion of the identified genes (44%) and proteins (29%) were unannotated in our analysis indicates that the complete role that AdeN plays in the cell remains unclear and will require further study. Global-omics were validated by comparison of the two data sets. Of the identified 31 significantly changed proteins identified by proteomics 29 were identified in the RNA-Seq analysis however only 6 showed a statistically significant change at the RNA level. This includes the AdeIJK efflux pump as anticipated.

Most prominent were the genes that encode proteins involved in oxidation-reduction processes, metabolic processes, and membrane proteins. For example, we found that *csuB* (A1S_2216) was not detected in AB141 (Appendix 9.3.1). In addition to controlling biofilm establishment, CsuB is also involved in pili-dependent twitching motility in *A. baumannii* (Tomaras et al. 2003). Therefore, reduced biofilm formation as well as motility in AB141 could be explained by the downregulation of *csu* operon.

Among the genes involved in oxidation-reduction processes, we observed upregulation of the catalase-encoding *katG* (A1S_1386). KatG is involved in protection against oxidative stress and its overexpression upon *adeN* deletion may mimic conditions to oxidative stress for *A. baumannii* ATCC17978. However, the potential link between AdeN and oxidative stress requires further investigation.

We also observed upregulation of the *paa* operon (both by transcriptomic and proteomic approaches) which is involved in the phenylacetic acid metabolism. Recently it was shown that the overexpression of the phenylacetic acid metabolism pathway in *A. baumannii* causes increased virulence in a zebra fish model by preventing the recruitment of neutrophils to the infection site (Bhuiyan et al. 2016). However, we observed that AB141 displayed reduced virulence in *G. mellonella* (Fig. 10), despite the over expression of *paa* operon. This could be due to two possible reasons, (1) that the role of *paa* in virulence may be host specific, or (2) that the presence of other proteins like those coded by the *csu* operon is more specific for the virulence of *A. baumannii* in *G. mellonella*.

Lastly scanning electron microscopy of the *adeN* and *adeIJK* deletion mutants (Fig. 13) shows a rounded cell morphotype in the *adeIJK* deletion mutants, AB185 and AB186, that is contrary to the rod shaped morphotype shown in the wild-type ATCC17978 and the *adeN* deletion mutant AB141. This indicates that the AdeIJK efflux pump, the only conserved and constitutively expressed pump in *A. baumannii*, plays a role in the cellular structure of *A. baumannii*.

6 Conclusions

To summarize, using transcriptomic and proteomic approaches, we show that AdeN likely regulates the expression of a much wider array of genes than previously thought. We also show that the deletion of *adeN* not only impacts the antibiotic resistance of *A. baumannii* due to upregulation of the AdeIJK pump as previously shown, but plays a larger role in *A. baumannii*. AdeN deletion was shown to attenuate virulence, in a *G. mellonella* model, as well as virulence associated phenotypes including cell motility and biofilm formation in addition of other cellular functions such as membrane lipid composition and osmotic stress tolerance. Thus, our data suggests that AdeN may be playing global role in regulating the virulence and antibiotic resistance of *A. baumannii*. Our findings also indicate that while the resistance associated phenotypes tested, antibiotic susceptibility and osmotic stress tolerance, are AdeIJK dependent, virulence associated phenotypes, biofilm formation, twitching motility, and virulence in *G. mellonella*, are AdeIJK independent. However this work also suggests that the interaction between AdeN and the AdeIJK efflux pump is much more complex than previously thought and well require significant further study in order to elucidate.

7 Future Directions

The logical continuation of this work lies in elucidating the complex regulatory interactions between AdeN and the AdeIJK efflux pump. In addition to establishing the role of AdeN as a global regulator, this study also suggests a global impact of AdeIJK deletion on *A. baumannii*. Thus, the next steps would involve studying the metabolic and physiological function of the AdeIJK pump.

This can be studied in the same way as AdeN was studied by use of a multi-omics approach to study the global changes brought on by *adeIJK* deletion as well as study of the *adeN* and *adeIJK* double mutant. Combined transcriptomic and proteomic data sets from all three mutants could be used to determine which groups of genes are affected by *adeN* deletion and what can be contributed to *adeIJK* deletion. Again combining the global studies with phenotypic complementation studies utilizing the same single-copy insertion system used in this study. Complementation of AdeIJK and AdeN into AB185 (Δ*adeIJK*) and AB186 (Δ*adeN*Δ*adeIJK*) in addition to AB183 would give us system where using IPTG induction we can modulate expression of AdeN and AdeIJK both in the presence and absence of the other. Phenotypic testing using this system would allow us to determine conclusively what phenotypes are controlled exclusively by AdeN and which are dependent on the presence of AdeIJK. We would also be able to determine if any of the tested phenotypes are dependent on both AdeN and AdeIJK.

8 Bibliography

Abraham, E.P., and Chain, E. 1940. An enzyme from bacteria able to destroy penicillin. Rev. Infect. Dis. **10**(4): 677–8.

Afgan, E., Baker, D., van den Beek, M., Blankenberg, D., Bouvier, D., Čech, M., Chilton, J., Clements, D., Coraor, N., Eberhard, C., Grüning, B., Guerler, A., Hillman-Jackson, J., Von Kuster, G., Rasche, E., Soranzo, N., Turaga, N., Taylor, J., Nekrutenko, A., and Goecks, J. 2016. The Galaxy platform for accessible, reproducible and collaborative biomedical analyses: 2016 update. Nucleic Acids Res. **44**(W1): W3–W10.

Ahn, S.K., Cuthbertson, L., and Nodwell, J.R. 2012. Genome Context as a Predictive Tool for Identifying Regulatory Targets of the TetR Family Transcriptional Regulators. PLoS One **7**(11): e50562.

Aminov, R.I. 2010. A brief history of the antibiotic era: lessons learned and challenges for the future. Front. Microbiol. **1**: 134.

Aminov, R.I., and Mackie, R.I. 2007. Evolution and ecology of antibiotic resistance genes. FEMS Microbiol. Lett. **271**(2): 147–161.

Antibiotic Resistance Threats in the United States. 2013. Available from https://www.cdc.gov/drugresistance/threat-report-2013/

Apisarnthanarak, A., and Mundy, L.M. 2009. Mortality associated with Pandrug-resistant *Acinetobacter baumannii* infections in Thailand. Am. J. Infect. Control **37**(6): 519–20.

Bassett, E.J., Keith, M.S., Armelagos, G.J., Martin, D.L., and Villanueva, A.R. 1980. Tetracycline-labeled human bone from ancient Sudanese Nubia (A.D. 350). Science **209**(4464): 1532–4.

Beck, C.F., Mutzel, R., Barbé, J., and Müller, W. 1982. A multifunctional gene (tetR) controls Tn10-encoded tetracycline resistance. J. Bacteriol. **150**(2): 633–42.

Bhuiyan, M.S., Ellett, F., Murray, G.L., Kostoulias, X., Cerqueira, G.M., Schulze, K.E., Mahamad Maifiah, M.H., Li, J., Creek, D.J., Lieschke, G.J., and Peleg, A.Y. 2016. *Acinetobacter baumannii* phenylacetic acid metabolism influences infection outcome through a direct effect on neutrophil chemotaxis. Proc. Natl. Acad. Sci. U. S. A. **113**(34): 9599–604.

Bou, G., Cerveró, G., Domínguez, M.A., Quereda, C., and Martínez-Beltrán, J. 2000. Characterization of a nosocomial outbreak caused by a multiresistant *Acinetobacter baumannii* strain with a carbapenem-hydrolyzing enzyme: high-level carbapenem resistance in *A. baumannii* is not due solely to the presence of beta-lactamases. J. Clin. Microbiol. **38**(9): 3299–305.

Catel-Ferreira, M., Coadou, G., Molle, V., Mugnier, P., Nordmann, P., Siroy, A., Jouenne, T., and Dé, E. 2011. Structure–function relationships of CarO, the carbapenem resistance-associated outer membrane protein of *Acinetobacter baumannii*. J. Antimicrob. Chemother. **66**(9): 2053–2056.

Cha, J.Y., Ishiwata, A., and Mobashery, S. 2004. A Novel β-Lactamase Activity from a Penicillin-binding Protein of *Treponema pallidum* and Why Syphilis Is Still Treatable with Penicillin. J. Biol. Chem. **279**(15): 14917–14921.

Chain, E., Florey, H.W., Gardner, A.D., Heatley, N.G., Jennings, M.A., Orr-Ewing, J., and Sanders, A.G. 1940. Penicillin As A Chemotherapeutic Agent. Lancet **236**(6104): 226–228.

Choi, K.-H., Gaynor, J.B., White, K.G., Lopez, C., Bosio, C.M., Karkhoff-Schweizer, R.R., and Schweizer, H.P. 2005. A Tn7-based broad-range bacterial cloning and expression system. Nat. Methods **2**(6): 443–448.

Choi, K.-H., and Schweizer, H.P. 2005. An improved method for rapid generation of unmarked

Pseudomonas aeruginosa deletion mutants. BMC Microbiol. **5**: 30.

Choi, K.-H., and Schweizer, H.P. 2006. mini-Tn7 insertion in bacteria with single attTn7 sites: example *Pseudomonas aeruginosa*. Nat. Protoc. **1**(1): 153–61..

Chuang, Y.-Y., Huang, Y.-C., Lin, C.-H., Su, L.-H., and Wu, C.-T. 2009. Epidemiological investigation after hospitalising a case with pandrug-resistant *Acinetobacter baumannii* infection. J. Hosp. Infect. **72**(1): 30–5.

Clinical and Laboratory Standards Institute. 2012. Methods for Dilution Antimicrobial Susceptibility Tests for Bacteria That Grow Aerobically ; Approved Standard — Ninth Edition. *In* Methods for Dilution Antimicrobial Susceptibility Tests for Bacteria That Grow Aerobically; Approved Standar- Ninth Edition.

Cook, M., Molto, E., and Anderson, C. 1989. Fluorochrome labelling in roman period skeletons from dakhleh oasis, Egypt. Am. J. Phys. Anthropol. **80**(2): 137–143.

Coyne, S., Rosenfeld, N., Lambert, T., Courvalin, P., and Périchon, B. 2010. Overexpression of resistance-nodulation-cell division pump AdeFGH confers multidrug resistance in *Acinetobacter baumannii*. Antimicrob. Agents Chemother. **54**(10): 4389–93.

Cui, L., and Su, X. 2009. Discovery, mechanisms of action and combination therapy of artemisinin. Expert Rev. Anti. Infect. Ther. **7**(8): 999–1013.

Cuthbertson, L., and Nodwell, J.R. 2013. The TetR family of regulators. Microbiol. Mol. Biol. Rev. **77**(3): 440–75.

Dale, J.W., and Greenaway, P.J. 1984. Bacterial Transformation (Kushner Method). *In* Nucleic Acids. Humana Press, New Jersey. pp. 241–244.

Damier-Piolle, L., Magnet, S., Brémont, S., Lambert, T., and Courvalin, P. 2008a. AdeIJK, a resistance-nodulation-cell division pump effluxing multiple antibiotics in *Acinetobacter*

baumannii. Antimicrob. Agents Chemother. **52**(2): 557–62.

Damier-Piolle, L., Magnet, S., Brémont, S., Lambert, T., and Courvalin, P. 2008b. AdeIJK, a resistance-nodulation-cell division pump effluxing multiple antibiotics in *Acinetobacter baumannii*. Antimicrob. Agents Chemother. **52**(2): 557–62.

Ehrlich, P., and Hata, S. 1910. Die experimentelle Chemotherapie der Spirillosen. Berlin **Julius Spr**.

Emmerich, R., and Löw, O. 1899. Bakteriolytische Enzyme als Ursache der erworbenen Immunität und die Heilung von Infectionskrankheiten durch dieselben. Zeitschrift für Hyg. und Infect. **31**(1): 1–65.

Falkinham, J.O., Wall, T.E., Tanner, J.R., Tawaha, K., Alali, F.Q., Li, C., and Oberlies, N.H. 2009. Proliferation of Antibiotic-Producing Bacteria and Concomitant Antibiotic Production as the Basis for the Antibiotic Activity of Jordan's Red Soils. Appl. Environ. Microbiol. **75**(9): 2735–2741.

Fernando, D.M., Chong, P., Singh, M., Spicer, V., Unger, M., Loewen, P.C., Westmacott, G., and Kumar, A. 2017. Multi-omics approach to study global changes in a triclosan-resistant mutant strain of *Acinetobacter baumannii* ATCC 17978. Int. J. Antimicrob. Agents **49**(1): 74–80.

Fernando, D.M., Xu, W., Loewen, P.C., Zhanel, G.G., and Kumar, A. 2014. Triclosan can select for an AdeIJK-overexpressing mutant of *Acinetobacter baumanni*i ATCC 17978 that displays reduced susceptibility to multiple antibiotics. Antimicrob. Agents Chemother. **58**(11): 6424–31.

Gaddy, J.A., Arivett, B.A., McConnell, M.J., López-Rojas, R., Pachón, J., and Actis, L.A. 2012. Role of acinetobactin-mediated iron acquisition functions in the interaction of *Acinetobacter*

baumannii strain ATCC 19606T with human lung epithelial cells, *Galleria mellonella* caterpillars, and mice. Infect. Immun. **80**(3): 1015–24.

Gehrlein, M., Leying, H., Cullmann, W., Wendt, S., and Opferkuch, W. 1991. Imipenem resistance in *Acinetobacter baumanii* is due to altered penicillin-binding proteins. Chemotherapy **37**(6): 405–12.

Gennis, R.B. 1989. Biomembranes; Molecular Structure and Function. Springer New York, New York, NY.

Gordon, N.C., and Wareham, D.W. 2010. Multidrug-resistant *Acinetobacter baumannii*: mechanisms of virulence and resistance. Int. J. Antimicrob. Agents **35**(3): 219–26.

Hamad, M.A., Zajdowicz, S.L., Holmes, R.K., and Voskuil, M.I. 2009. An allelic exchange system for compliant genetic manipulation of the select agents *Burkholderia pseudomallei* and *Burkholderia mallei*. Gene **430**(1–2): 123–131.

Harding, C.M., Tracy, E.N., Carruthers, M.D., Rather, P.N., Actis, L.A., and Munson, R.S. 2013. *Acinetobacter baumannii* strain M2 produces type IV pili which play a role in natural transformation and twitching motility but not surface-associated motility. MBio **4**(4): e00360-13.

Higgins, P.G., Wisplinghoff, H., Stefanik, D., and Seifert, H. 2004. Selection of topoisomerase mutations and overexpression of adeB mRNA transcripts during an outbreak of *Acinetobacter baumannii*. J. Antimicrob. Chemother. **54**(4): 821–823.

Hoang, T.T., Karkhoff-Schweizer, R.R., Kutchma, A.J., and Schweizer, H.P. 1998. A broad-host-range Flp-FRT recombination system for site-specific excision of chromosomally-located DNA sequences: application for isolation of unmarked *Pseudomonas aeruginosa* mutants. Gene **212**(1): 77–86.

Hou, P.F., Chen, X.Y., Yan, G.F., Wang, Y.P., and Ying, C.M. 2012. Study of the Correlation of Imipenem Resistance with Efflux Pumps AdeABC, AdeIJK, AdeDE and AbeM in Clinical Isolates of *Acinetobacter baumannii*. Chemotherapy **58**(2): 152–158.

Iwashkiw, J.A., Seper, A., Weber, B.S., Scott, N.E., Vinogradov, E., Stratilo, C., Reiz, B., Cordwell, S.J., Whittal, R., Schild, S., and Feldman, M.F. 2012. Identification of a general O-linked protein glycosylation system in *Acinetobacter baumannii* and its role in virulence and biofilm formation. PLoS Pathog. **8**(6): e1002758.

Jain, R., and Danziger, L.H. 2004. Multidrug-resistant *Acinetobacter* infections: an emerging challenge to clinicians. Ann. Pharmacother. **38**(9): 1449–59.

Jasovský, D., Littmann, J., Zorzet, A., and Cars, O. 2016. Antimicrobial resistance-a threat to the world's sustainable development. Ups. J. Med. Sci. **121**(3): 159–64.

Kobayashi, T., Nonaka, L., Maruyama, F., and Suzuki, S. 2007. Molecular Evidence for the Ancient Origin of the Ribosomal Protection Protein That Mediates Tetracycline Resistance in Bacteria. J. Mol. Evol. **65**(3): 228–235.

Kumar, A., Dalton, C., Cortez-Cordova, J., and Schweizer, H.P. 2010. Mini-Tn7 vectors as genetic tools for single copy gene cloning in *Acinetobacter baumannii*. J. Microbiol. Methods **82**(3): 296–300.

Kumar, A., and Schweizer, H.P. 2005. Bacterial resistance to antibiotics: Active efflux and reduced uptake. Adv. Drug Deliv. Rev. **57**(10): 1486–1513.

Kumarasamy, K.K., Toleman, M.A., Walsh, T.R., Bagaria, J., Butt, F., Balakrishnan, R., Chaudhary, U., Doumith, M., Giske, C.G., Irfan, S., Krishnan, P., Kumar, A. V, Maharjan, S., Mushtaq, S., Noorie, T., Paterson, D.L., Pearson, A., Perry, C., Pike, R., Rao, B., Ray, U., Sarma, J.B., Sharma, M., Sheridan, E., Thirunarayan, M.A., Turton, J., Upadhyay, S.,

Warner, M., Welfare, W., Livermore, D.M., and Woodford, N. 2010. Emergence of a new antibiotic resistance mechanism in India, Pakistan, and the UK: a molecular, biological, and epidemiological study. Lancet. Infect. Dis. **10**(9): 597–602.

Langmead, B., and Salzberg, S.L. 2012. Fast gapped-read alignment with Bowtie 2. Nat. Methods **9**(4): 357–359.

Lewis, K. 2013. Platforms for antibiotic discovery. Nat. Rev. Drug Discov. **12**(5): 371–387.

Lin, M.-F., and Lan, C.-Y. 2014. Antimicrobial resistance in *Acinetobacter baumannii* : From bench to bedside. World J. Clin. Cases **2**(12): 787.

Magnet, S., Courvalin, P., and Lambert, T. 2001. Resistance-nodulation-cell division-type efflux pump involved in aminoglycoside resistance in *Acinetobacter baumannii* strain BM4454. Antimicrob. Agents Chemother. **45**(12): 3375–80.

Marchand, I., Damier-Piolle, L., Courvalin, P., and Lambert, T. 2004. Expression of the RND-Type Efflux Pump AdeABC in *Acinetobacter baumannii* Is Regulated by the AdeRS Two-Component System. Antimicrob. Agents Chemother. **48**(9): 3298–3304.

Michalopoulos, A., and Falagas, M.E. 2010. Treatment of *Acinetobacter* infections. Expert Opin. Pharmacother. **11**(5): 779–88.

Moffatt, J.H., Harper, M., Harrison, P., Hale, J.D.F., Vinogradov, E., Seemann, T., Henry, R., Crane, B., St. Michael, F., Cox, A.D., Adler, B., Nation, R.L., Li, J., and Boyce, J.D. 2010. Colistin Resistance in *Acinetobacter baumannii* Is Mediated by Complete Loss of Lipopolysaccharide Production. Antimicrob. Agents Chemother. **54**(12): 4971–4977.

Mohammad, I., Hsien, T., and Lee, K. 2013. A method for generating marker-less gene deletions in multidrug-resistant *Acinetobacter baumannii*. BMC Microbiol. **13**: 1.

Nelson, M.L., Dinardo, A., Hochberg, J., and Armelagos, G.J. 2010. Brief communication: Mass

spectroscopic characterization of tetracycline in the skeletal remains of an ancient population from Sudanese Nubia 350-550 CE. Am. J. Phys. Anthropol. **143**(1): 151–154.

O'Neill, J. 2014. Antimicrobial Resistance: Tackling a crisis for the health and wealth of nations The Review on Antimicrobial Resistance Chaired.

Peleg, A.Y., Seifert, H., and Paterson, D.L. 2008. *Acinetobacter baumannii*: emergence of a successful pathogen. Clin. Microbiol. Rev. **21**(3): 538–82.

Perez, F., Hujer, A.M., Hujer, K.M., Decker, B.K., Rather, P.N., and Bonomo, R.A. 2007. Global Challenge of Multidrug-Resistant *Acinetobacter baumannii*. Antimicrob. Agents Chemother. **51**(10): 3471–3484.

Pfaffl, M.W. 2001. A new mathematical model for relative quantification in real-time RT-PCR. Nucleic Acids Res. **29**(9): e45.

Quale, J., Bratu, S., Landman, D., and Heddurshetti, R. 2003. Molecular Epidemiology and Mechanisms of Carbapenem Resistance in *Acinetobacter baumannii* Endemic in New York City. Clin. Infect. Dis. **37**(2): 214–220.

Reichheld, S.E., Yu, Z., and Davidson, A.R. 2009. The induction of folding cooperativity by ligand binding drives the allosteric response of tetracycline repressor. Proc. Natl. Acad. Sci. **106**(52): 22263–22268.

Ribera, A., Ruiz, J., and Vila, J. 2003. Presence of the Tet M determinant in a clinical isolate of *Acinetobacter baumannii*. Antimicrob. Agents Chemother. **47**(7): 2310–2.

Rollo, I.M., Williamson, J., and Plackett, R.L. 1952. Acquired resistance to penicillin and to neoarsphenamine in *Spirochaeta recurrentis*. Br. J. Pharmacol. Chemother. **7**(1): 33–41.

Rosenfeld, N., Bouchier, C., Courvalin, P., and Périchon, B. 2012. Expression of the resistance-nodulation-cell division pump AdeIJK in *Acinetobacter baumannii* is regulated by AdeN, a

TetR-type regulator. Antimicrob. Agents Chemother. **56**(5): 2504–10.

Ruzin, A., Keeney, D., and Bradford, P.A. 2007. AdeABC multidrug efflux pump is associated with decreased susceptibility to tigecycline in *Acinetobacter calcoaceticus-Acinetobacter baumannii* complex. J. Antimicrob. Chemother. **59**(5): 1001–1004.

Saranathan, R., Pagal, S., Sawant, A.R., Tomar, A., Madhangi, M., Sah, S., Satti, A., Arunkumar, K.P., and Prashanth, K. 2017. Disruption of tetR type regulator *adeN* by mobile genetic element confers elevated virulence in *Acinetobacter baumannii*. Virulence: 1–19.

Schweizer, H.P. 1991. The agmR gene, an environmentally responsive gene, complements defective glpR, which encodes the putative activator for glycerol metabolism in *Pseudomonas aeruginosa*. J. Bacteriol. **173**(21): 6798.

Smani, Y., Fabrega, A., Roca, I., Sanchez-Encinales, V., Vila, J., and Pachon, J. 2014. Role of OmpA in the Multidrug Resistance Phenotype of *Acinetobacter baumannii*. Antimicrob. Agents Chemother. **58**(3): 1806–1808.

Tien, H.C., Battad, A., Bryce, E.A., Fuller, J., Mulvey, M., Bernard, K., Brisebois, R., Doucet, J.J., Rizoli, S.B., Fowler, R., and Simor, A. 2007. Multi-drug resistant *Acinetobacter* infections in critically injured Canadian forces soldiers. BMC Infect. Dis. **7**: 95.

Tomaras, A.P., Dorsey, C.W., Edelmann, R.E., and Actis, L.A. 2003. Attachment to and biofilm formation on abiotic surfaces by *Acinetobacter baumannii*: involvement of a novel chaperone-usher pili assembly system. Microbiology **149**(12): 3473–3484.

Tomas, M. d. M., Beceiro, A., Perez, A., Velasco, D., Moure, R., Villanueva, R., Martinez-Beltran, J., and Bou, G. 2005. Cloning and Functional Analysis of the Gene Encoding the 33- to 36-Kilodalton Outer Membrane Protein Associated with Carbapenem Resistance in *Acinetobacter baumannii*. Antimicrob. Agents Chemother. **49**(12): 5172–5175.

Trapnell, C., Williams, B.A., Pertea, G., Mortazavi, A., Kwan, G., van Baren, M.J., Salzberg, S.L., Wold, B.J., and Pachter, L. 2010. Transcript assembly and quantification by RNA-Seq reveals unannotated transcripts and isoform switching during cell differentiation. Nat. Biotechnol. **28**(5): 511–515.

Vila, J., Ruiz, J., Goñi, P., Marcos, A., and Jimenez de Anta, T. 1995. Mutation in the gyrA gene of quinolone-resistant clinical isolates of *Acinetobacter baumannii*. Antimicrob. Agents Chemother. **39**(5): 1201–3.

Watkins, R.R., and Bonomo, R.A. 2016. Overview: Global and Local Impact of Antibiotic Resistance. Infect. Dis. Clin. North Am. **30**(2): 313–322.

WHO | Global priority list of antibiotic-resistant bacteria to guide research, discovery, and development of new antibiotics. 2017. *In* WHO. World Health Organization.

Wong, R.W.K., Hägg, U., Samaranayake, L., Yuen, M.K.Z., Seneviratne, C.J., and Kao, R. 2010. Antimicrobial activity of Chinese medicine herbs against common bacteria in oral biofilm. A pilot study. Int. J. Oral Maxillofac. Surg. **39**(6): 599–605.

Yoon, E.-J., Courvalin, P., and Grillot-Courvalin, C. 2013. RND-Type Efflux Pumps in Multidrug-Resistant Clinical Isolates of *Acinetobacter baumannii*: Major Role for AdeABC Overexpression and AdeRS Mutations. Antimicrob. Agents Chemother. **57**(7): 2989–2995.

Yu, Z., Reichheld, S.E., Savchenko, A., Parkinson, J., and Davidson, A.R. 2010. A Comprehensive Analysis of Structural and Sequence Conservation in the TetR Family Transcriptional Regulators. J. Mol. Biol. **400**(4): 847–864.

Zhu, J., Wang, C., Wu, J., Jiang, R., Mi, Z., and Huang, Z. 2009. A novel aminoglycoside-modifying enzyme gene aac(6′)-Ib in a pandrug-resistant *Acinetobacter baumannii* strain. J. Hosp. Infect. **73**(2): 184–185.

9 Appendices

9.1 Sequencing Data

9.1.1 AB141 *adeN* sequencing

Upstream and downstream regions are underlined. Flp-recombinase scar is bolded and remaining adeN sequence is given in italics. Junk sequence is given in lower-case

ACTTTGTCAGAAGCTTAAAACCGAAGCAAAAATCAAAAAGCGGCTAATTTAATTTA
GCCGCTTTTCTTTATGACTATTTAAAACGGAATTAACTGCCAAACTAAAATGTGAAC
ATACAGTTACATGATCAAAAAATTCTAAATTTCTACATAACTCATTATATTTTCTATA
TTTCCCCCAAAACTATGCTCTACTTATTGTTTACCAGATGACCTAAAAACATACCAAT
GACCATCGTTAAAGATAGATTTGCTATACTAGATAAGCAGTGTTAGCCGTCGTTATT
AAATTTT*ATGA*cgaattagcttcaaaagcgctct**GAAGTTCCTATACTTTCTAGAGAATAGGAAC**
TTCGGAATAGGAACTTCaagatccccaattcg*TAA*TTCTTTTGCATTTTGAAATGCTTATAGT
ATAGTAGACTTCTTTTTTCCCACTTCCACCCAGCCAACAACAGATAATTGTTGTAATT
CAAAACAATTATTATGGAGTAGCTACATGGCTCTAAGACATTTCCTGACTTTACGTG
ATCTATCCACTCTAGAACTTAATCGCATTTTGGAACGCGCAAGCGAACTTAAGAAAA
TGCAGCAAAGCAATAAGGTATATCAACCTTTTGTTGGTAAAGTA

9.1.2 AB185 *adeIJK* sequencing

Upstream and downstream regions are underlined. Flp-recombinase scar is bolded and remaining *adeIJK* sequence is given in italics. Junk sequence is given in lower-case

TCACGACCCACATGCTTACTACGAACAGTGCTTCCGTAAACGACATCAAGCTGCTTT
AAAATTTGGTGGCCTGGAACACTTTCTAAATTACTTAATAACATTGTTTTTTATCAAT
CTAAATTTCTTTAGCTTTCAAGATAAAAAATATTCAGATGAGTTGCAATAAAAAAGC
CCACCGAAGTGAGCTTTTATAAGAAAGTGATTTAAAACTTATTGCTTTTTAAGTTCA
GCACTAGAT*cgaattggggatcttgaagttcct***ATTCCGAAGTTCCTATTCTCTAGAAAGTATAG**
GAACTTC*agagcgcttttgaagctaattcg*
TTCACGAACATAGCTTCCTTCAGCAAATAAGCGTTTTAA
AATCACGCCACTTGTCTGAGGACGAACTTCAGAAATTTGATATGCTGAAGTACGGCCTGAA
AGCTCAACGCTTTGTTCAACACTTTGTGGTTGAGCAACAATAACACCTACTTCTGCAGGCG
GCATTTTCTGAGCAGCAGCAGCTTGCTGTTTCTCATCGGAGCCTTTGCTACAACCAACAAG
CGCGATACTTGTTGCTAATGCGCAAGCAGTAAGGGCTGGTGCCCAAAGCTTAGCCGACAT
*CAT*TGTTCCACCTCGTTTAGATAAAATCTAAAAATATA

9.1.3 AB186 *adeIJK* sequencing

Upstream and downstream regions are underlined. Flp-recombinase scar is bolded and remaining *adeIJK* sequence is given in italics. Junk sequence is given in lower-case

AGTCACGACCCACATGCTTACTACGAACAGTGCTTCCGTAAACGACATCAAGCTGCT
TTAAAATTTGGTGGCCTGGAACACTTTCTAAATTACTTAATAACATTGTTTTTTATCA
ATCTAAATTTCTTTAGCTTTCAAGATAAAAAATATTCAGATGAGTTGCAATAAAAAA
GCCCACCGAAGTGAGCTTTTATAAGAAAGTGATTTAAAACTTATTGCTTTTTAAGTT
CAGCACTAGATcgaattggggatcttgaagttcct**ATTCCGAAGTTCCTATTCTCTAGAAAGTAT**
AGGAACTTCagagcgcttttgaagctaattcg*TTCACGAACATAGCTTCCTTCAGCAAATAAGCGTTTT*
AAAATCACGCCACTTGTCTGAGGACGAACTTCAGAAATTTGATATGCTGAAGTACGGCCTG
AAAGCTCAACGCTTTGTTCAACACTTTGTGGTTGAGCAACAATAACACCTACTTCTGCAGG
CGGCATTTTCTGAGCAGCAGCAGCTTGCTGTTTCTCATCGGAGCCTTTGCTACAACCAACA
AGCGCGATACTTGTTGCTAATGCGCAAGCAGTAAGGGCTGGTGCCCAAAGCTTAGCCGAC
*ATCAT*TGTTCCACCTCGTTTAGATAAAATCTAAAAATATATT

9.2 Plasmid Maps

9.2.1 pPLS228

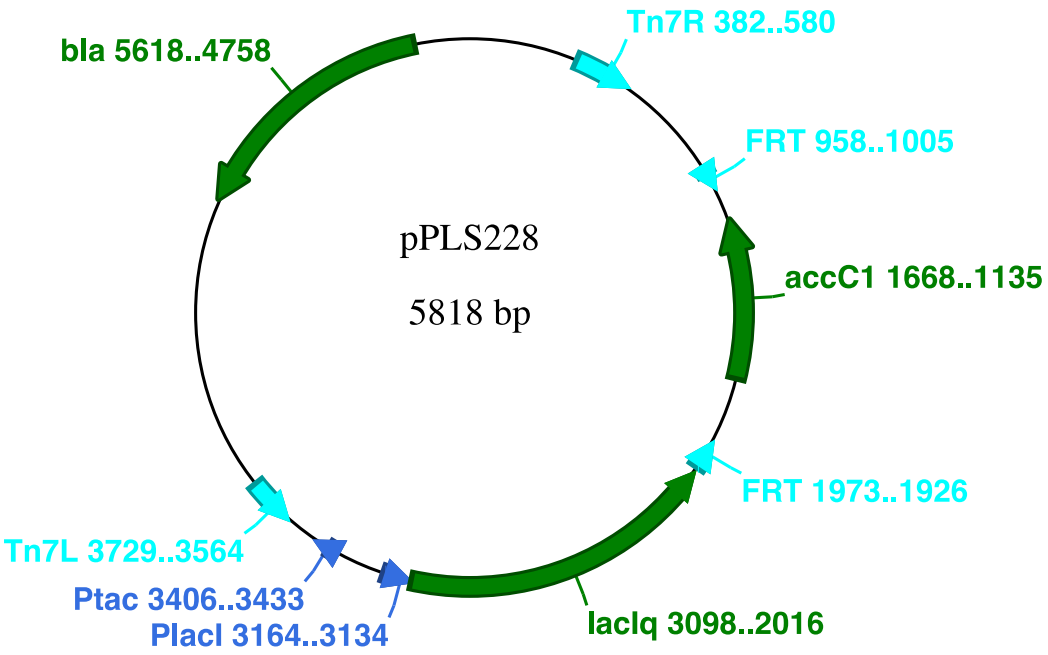

9.2.2 pPLS236

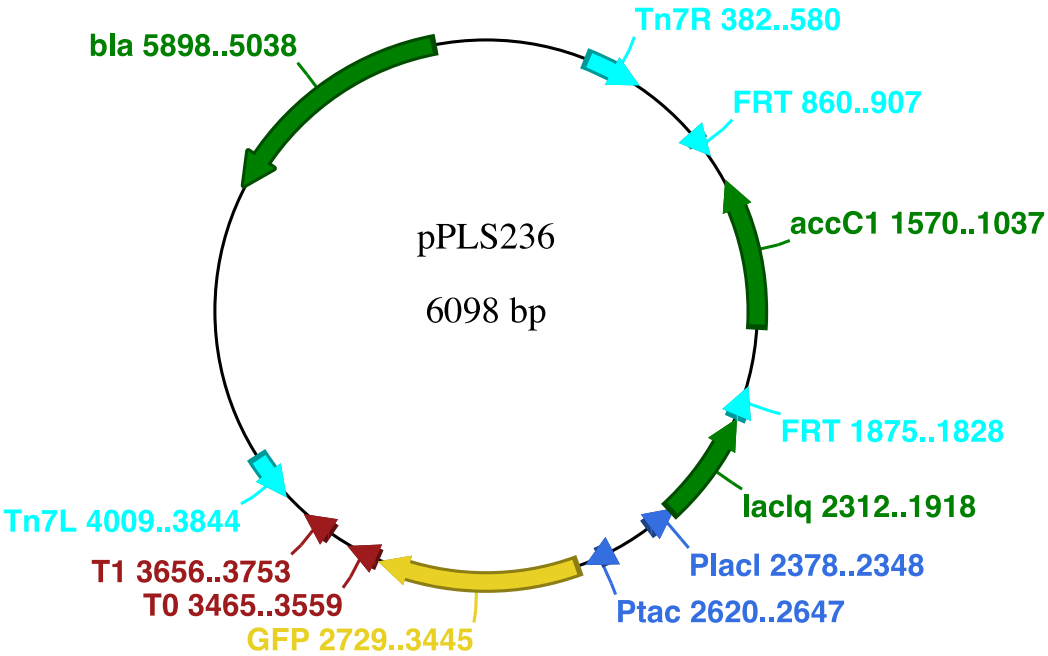

9.2.3 pPLS237

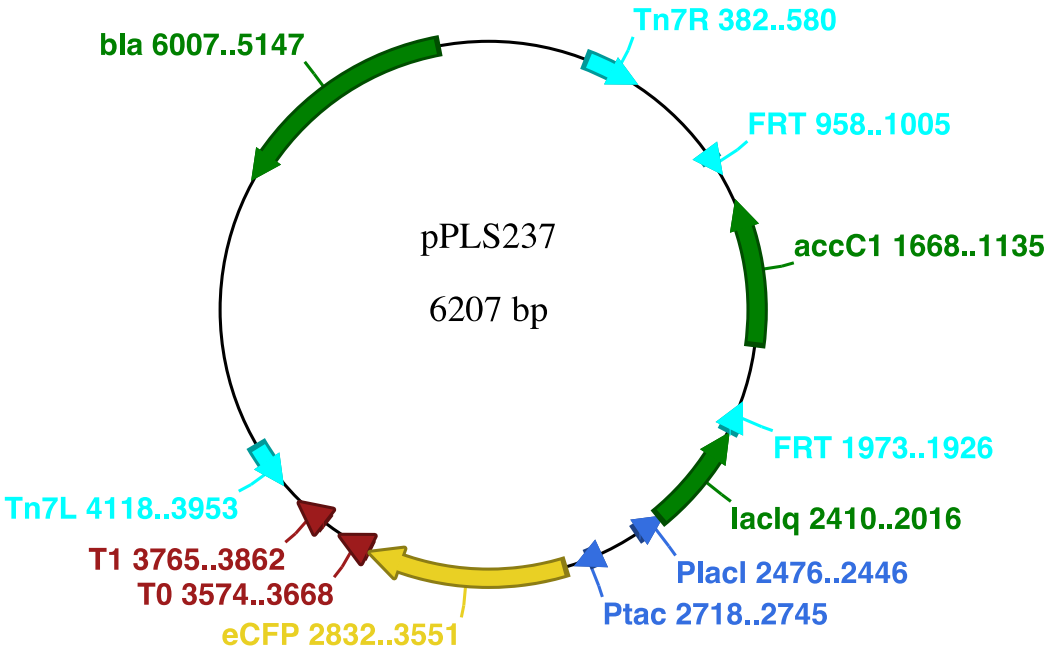

9.2.4 pPLS238

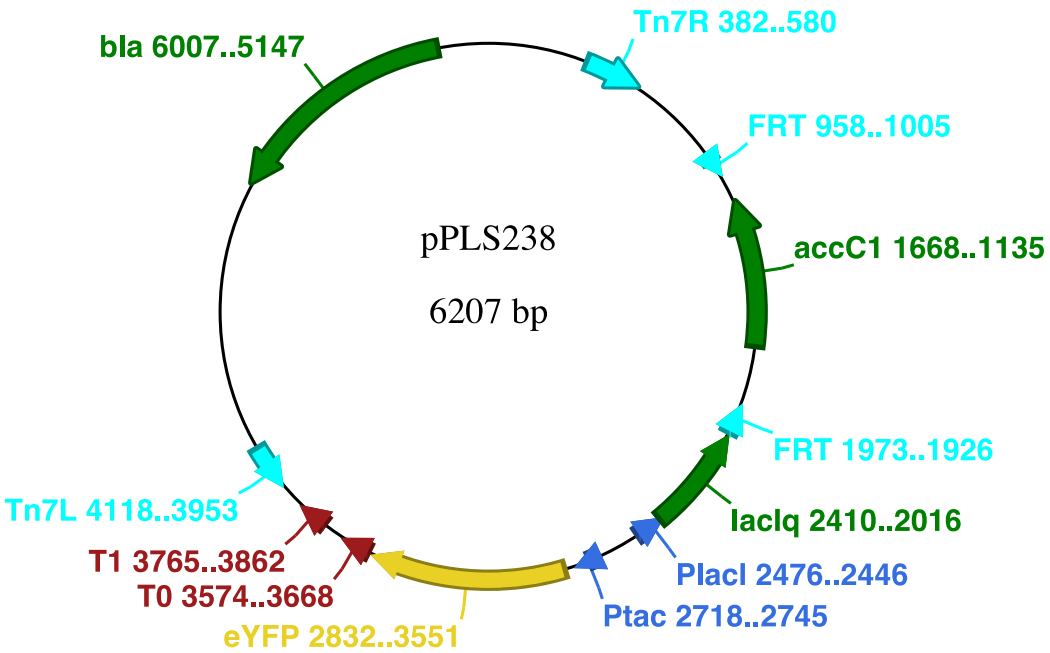

9.2.5 pPLS239

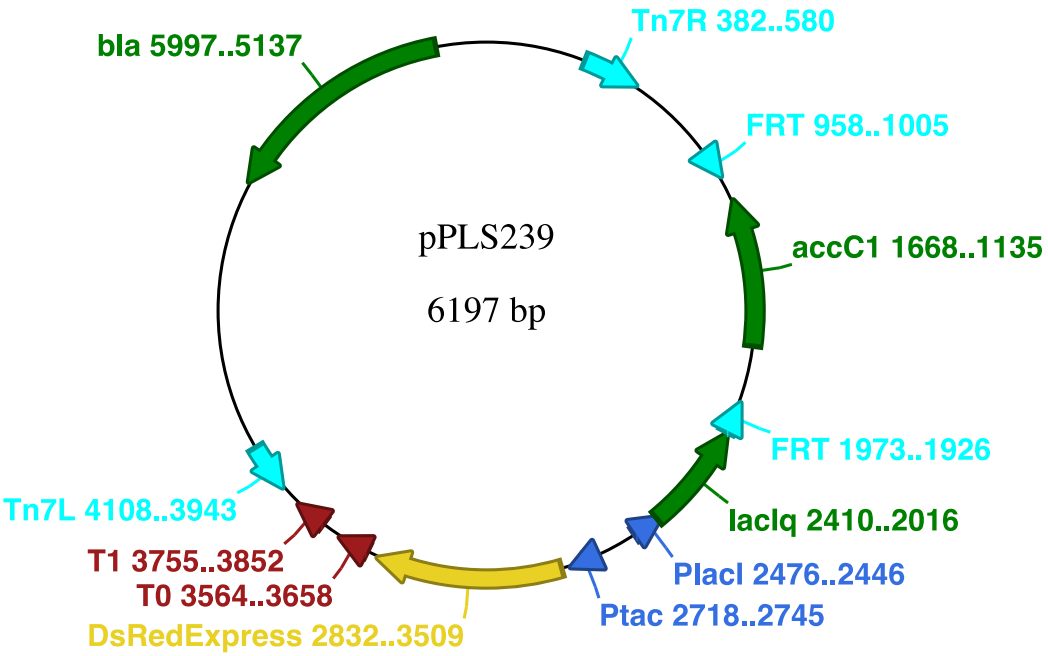
pPLS239
6197 bp
bla 5997..5137
Tn7R 382..580
FRT 958..1005
accC1 1668..1135
FRT 1973..1926
lacIq 2410..2016
PlacI 2476..2446
Ptac 2718..2745
DsRedExpress 2832..3509
T0 3564..3658
T1 3755..3852
Tn7L 4108..3943

9.3 RNA-Seq and Proteomics Supplemental Material

9.3.1 RNA-Seq Data Table

Gene	Fold change (log2)	Description
A1S_0067	-5.1	L-lactate permease
A1S_0068	-2.8	L-lactate utilization transcriptional repressor (GntR family)
A1S_0069	-3.4	L-lactate dehydrogenase
A1S_0070	-2.3	D-lactate dehydrogenase NADH independent, FAD-binding domain
A1S_0157	-1.9	hypothetical protein
A1S_0294	-1.6	contains frameshift; similar to chaperone Hsp90
A1S_0371	1.8	putative membrane protein
A1S_0384	inf	putative Zinc-binding protein
A1S_0466	-2.6	sec-independent protein translocase protein TatA
A1S_0741	2.7	hypothetical protein
A1S_0803	2.3	trehalose-6-phosphate synthase
A1S_0804	1.7	trehalose-6-phosphate phophatase
A1S_1013	-2.7	urease beta subunit
A1S_1093	1.4	Arginine/ornithine N-succinyltransferase beta subunit
A1S_1108	2.7	acyl coenzyme A dehydrogenase
A1S_1143	2.3	hypothetical protein
A1S_1146	2.2	site-specific DNA-methyltransferase
A1S_1147	2.2	Site-specific DNA methylase-like protein
A1S_1149	3.7	hypothetical protein
A1S_1256	3.1	putative transcriptional regulator
A1S_1260	-2.6	hypothetical protein
A1S_1275	2.7	hypothetical protein
A1S_1280	-1.6	transcriptional regulator DUF24 family
A1S_1312	1.8	peptidoglycan L-alanyl-D-glutamate endopeptidase CwlK
A1S_1327	-1.8	hypothetical protein
A1S_1335	3.7	Phenylacetic acid degradation protein paaN
A1S_1336	3.6	ring-1,2-phenylacetyl-CoA epoxidase subunit PaaA
A1S_1337	3.7	ring-1,2-phenylacetyl-CoA epoxidase subunit PaaB
A1S_1338	3.6	ring-1,2-phenylacetyl-CoA epoxidase subunit PaaC
A1S_1339	3.7	Phenylacetate-CoA oxygenase PaaJ subunit
A1S_1340	4.0	Phenylacetate-CoA oxygenase/reductase PaaK subunit
A1S_1341	4.2	Enoyl-CoA hydratase/carnithine racemase
A1S_1342	4.2	2-(1,2-epoxy-1,2-dihydrophenyl)acetyl-CoA isomerase

A1S_1343	4.3	3-hydroxybutyryl-CoA dehydrogenase
A1S_1344	4.2	Thiolase
A1S_1345	4.3	phenylacetate-CoA ligase
A1S_1346	4.0	phenylacetate-CoA ligase
A1S_1347	2.3	phenylacetic acid degradation operon negative regulatory protein
A1S_1348	2.3	phenylacetic acid degradation protein
A1S_1349	2.3	acyl-CoA thioesterase
A1S_1360	-1.6	ABC transporter
A1S_1384	1.8	nicotinamide-nucleotide amidase
A1S_1386	1.6	Catalase
A1S_1452	-4.2	arsenate reductase
A1S_1453	inf	ArsR family transcriptional regulator (aresenite inducible repressor)
A1S_1505	1.9	yyaM
A1S_1581	1.9	methyltransferase putative
A1S_1584	2.5	hypothetical protein
A1S_1586	2.3	EsvK1
A1S_1587	3.2	EsvK2
A1S_1588	2.4	Phage terminase-like protein large subunit
A1S_1590	2.8	peptidase U35 phage prohead HK97
A1S_1591	3.4	phage major capsid protein HK97
A1S_1592	3.7	putative Phage head-tail adaptor
A1S_1593	3.1	hypothetical protein
A1S_1594	3.1	hypothetical protein
A1S_1595	1.8	hypothetical protein
A1S_1596	2.1	hypothetical protein
A1S_1600	1.6	lysozyme
A1S_1622	-1.7	hypothetical protein
A1S_1658	1.6	putative hydrolase haloacid dehalogenase-like family
A1S_1699	2.0	pyruvate dehydrogenase E1 component alpha subunit
A1S_1700	1.9	pyruvate dehydrogenase E1 component beta subunit
A1S_1719	inf	4Fe-4S ferredoxin iron-sulfur binding
A1S_1736	1.7	putative membrane protein
A1S_1776	1.6	transcriptional regulatory protein
A1S_1844	-1.8	CatC3
A1S_1848	-2.6	Beta-ketoadipyl CoA thiolase
A1S_1869	1.5	putative porin for benzoate transport (BenP)
A1S_1931	1.9	hypothetical protein

A1S_1950	1.9	putative universal stress protein
A1S_1979	-inf	AdeN
A1S_2016	3.6	Phage-related lysozyme
A1S_2017	2.5	hypothetical protein
A1S_2018	2.1	tail tape meausure protein
A1S_2021	2.6	hypothetical protein
A1S_2022	2.6	putative tail fiber
A1S_2024	3.1	Glutamate 5-kinase
A1S_2025	3.0	hypothetical protein
A1S_2026	2.9	hypothetical protein
A1S_2027	3.2	hypothetical protein
A1S_2028	2.7	phage putative head morphogenesis protein
A1S_2029	2.9	hypothetical protein
A1S_2030	3.3	hypothetical protein putative phage associated protein
A1S_2031	4.8	hypothetical protein
A1S_2032	3.7	hypothetical protein
A1S_2035	1.9	hypothetical protein
A1S_2038	2.8	hypothetical protein
A1S_2039	2.7	hypothetical protein
A1S_2070	-1.6	P-type ATPase Mg2+ ATPase transporter
A1S_2183	1.8	putative signal peptide
A1S_2216	-inf	CsuB
A1S_2230	1.8	hypothetical protein
A1S_2299	-1.5	ABC transporter (histidine transport system ATP-binding protein)
A1S_2388	1.6	iron complex transport system permease protein
A1S_2389	-1.6	iron complex transport system permease protein
A1S_2449	3.8	aromatic amino acid transport protein AroP
A1S_2450	5.6	indolepyruvate decarboxylase
A1S_2452	3.6	NAD-dependent aldehyde dehydrogenase
A1S_2558	inf	putative transposase
A1S_2679	-1.7	hypothetical protein
A1S_2734	1.6	putative phosphatidylglycerophosphatase B
A1S_2736	1.7	RND family drug transporter AdeJ
A1S_2820	1.5	hypothetical protein
A1S_2823	1.6	hypothetical protein
A1S_3156	2.3	putative membrane protein

9.3.2 Proteomics Data Table

Gene	Fold change	Description
A1S_2450	3.8	putative pyruvate decarboxylase
A1S_1336	3.5	hypothetical protein
A1S_2736	3.2	RND family drug transporter, AdeJ
A1S_1466	3.2	glutaminase-asparaginase
A1S_2735	3.1	MF protein, AdeI
A1S_1340	2.6	Phenylacetate-CoA oxygenase/reductase PaaK subunit
A1S_2737	2.5	OM protein, AdeK
A1S_3132	2.3	succinylornithine transaminase
A1S_0062	2.2	putative UTP-glucose-1-phosphate uridylyltransferase
A1S_3131	2.1	arginine succinyltransferase
A1S_1000	2.0	sulfate adenylyltransferase subunit 2
A1S_2774	2.0	putative homoserine kinase (ThrH)
A1S_0140	1.9	NAD-linked malate dehydrogenase
A1S_1001	1.8	ATP-sulfurylase subunit 1
A1S_3129	1.7	succinylarginine dihydrolase
A1S_0474	1.6	putative ferric siderophore receptor protein
A1S_3180	-1.5	putative signal peptide
A1S_3175	-1.5	bacterioferritin
A1S_2462	-1.6	RNA helicase
A1S_3125	-1.6	putative signal peptide
A1S_1489	-1.6	putative glutathione S-transferase
A1S_0800	-1.6	bacterioferritin
A1S_0759	-1.6	NADH dehydrogenase I chain I 2Fe-2S ferredoxin-related
A1S_3185	-1.6	glutamate synthase large chain precursor
A1S_3317	-1.6	putative outer membrane protein
A1S_0157	-1.7	hypothetical protein
A1S_2848	-1.7	glucose dehydrogenase
A1S_1924	-1.9	cytochrome d terminal oxidase polypeptide subunit I
A1S_1925	-1.9	cytochrome d terminal oxidase polypeptide subunit II
A1S_0753	-2.0	NADH dehydrogenase I chain B
A1S_2820	-2.3	hypothetical protein